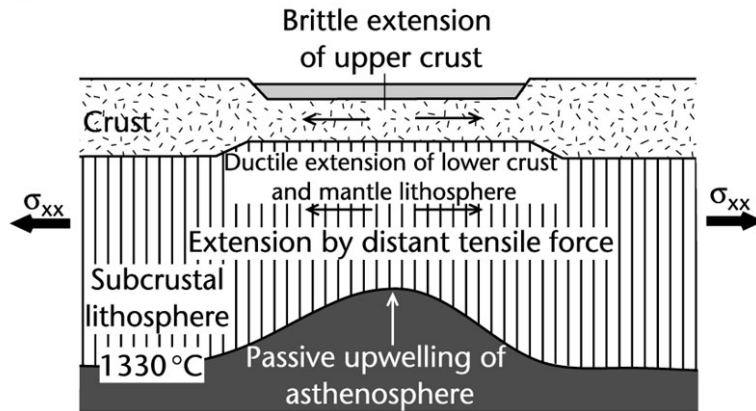


3.3 Introduction to models of continental extension

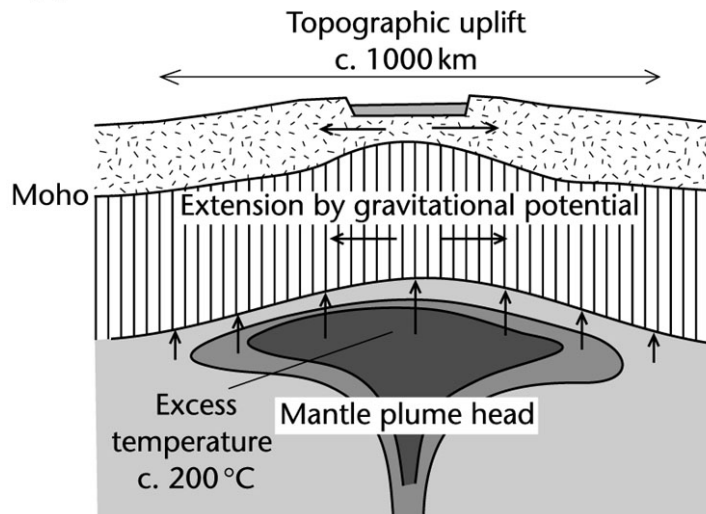
3.3.1 Active and passive rifting idealizations

(a) PASSIVE RIFTING



Passive rifting: Tensional stresses in the continental lithosphere cause it to fail, allowing hot mantle rocks to penetrate the lithosphere. Crustal doming and volcanic activity are only secondary processes.

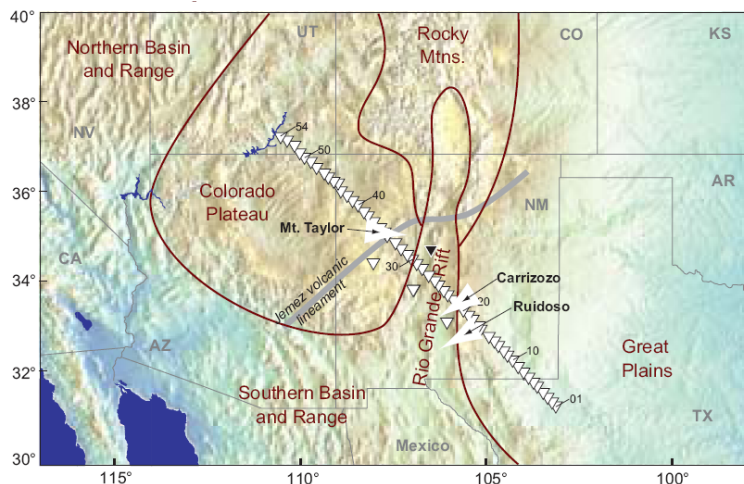
(b) ACTIVE RIFTING



Active rifting: associated with the impingement on the base of the lithosphere of a thermal plume or sheet. Conductive heating from the mantle plume, heat transfer from magma generation, or convective heating may cause the lithosphere to thin. If heat fluxes out of the asthenosphere are large enough, relatively rapid thinning of the continental lithosphere causes isostatic uplift. Tensional stresses generated by the uplift may then promote rifting.

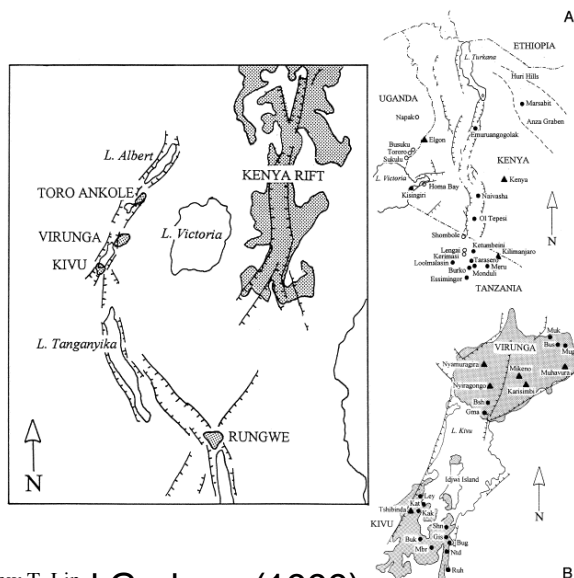
Fig. 3.10 Active and passive rifting end-member idealizations. (a) Passive rifting of the lithosphere and passive upwelling of hot asthenosphere; (b) Impingement on the base of the lithosphere of a mantle plume causes long wavelength topographic doming and gravitationally driven extension of the lithosphere.

Passive rifting example: Rio Grande rift



From: <http://www.aeic.alaska.edu/input/west/presentations/iris2003-miniposter.pdf>

Active rifting example: East African Rift system



Basin Analysis
Prepared by Dr. Andrew T. Lin
Furman and Graham (1999)
Dept. Earth Sci., Nat. Central Univ. Taiwan

Evidence for passive rifting

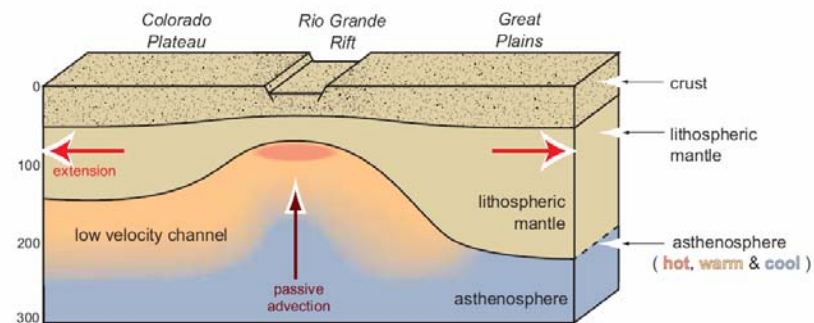
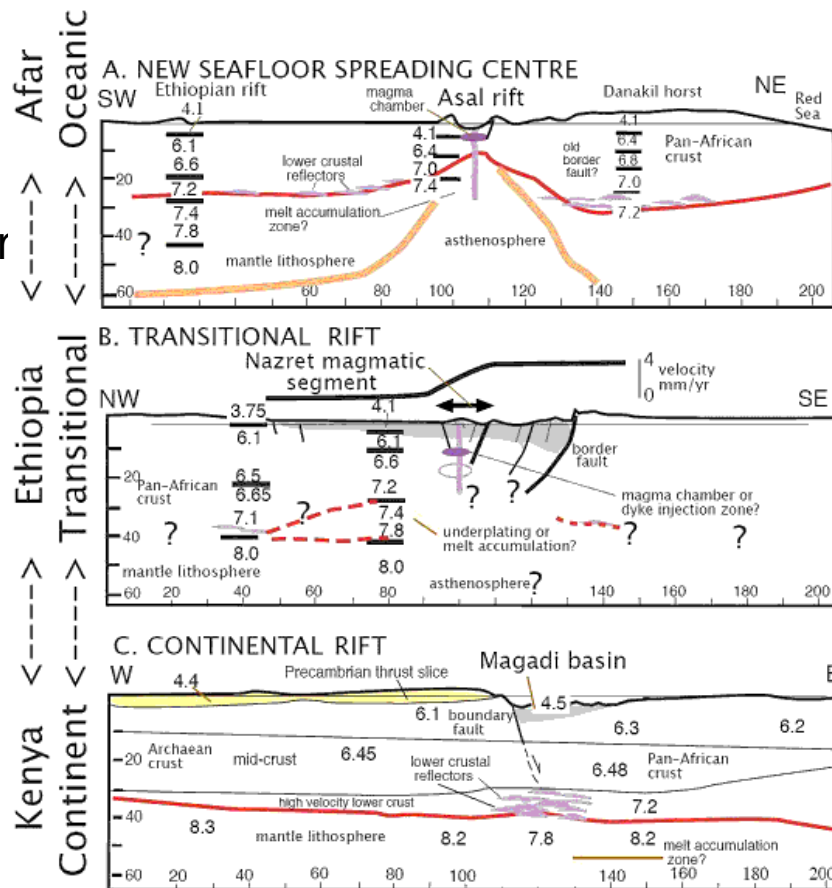
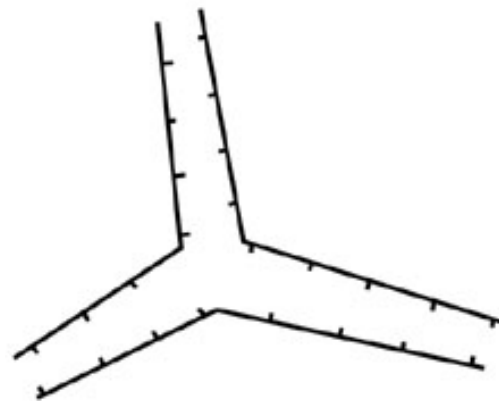


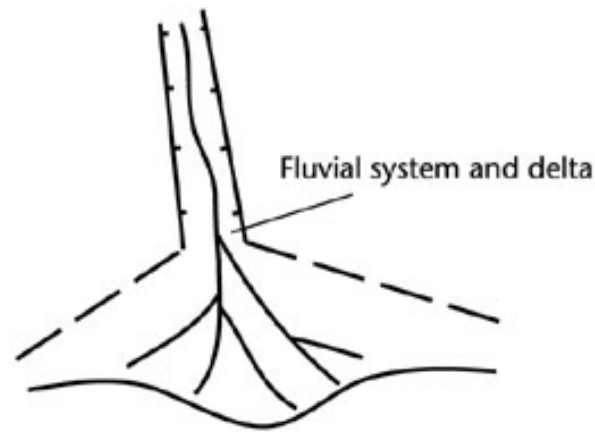
Figure 6. A symmetric region of low shear velocity is centered on the rift. Velocities as low as 4.2 km/s are found at depths of 55-90 km, consistent with a thin carapace of mantle lithosphere.



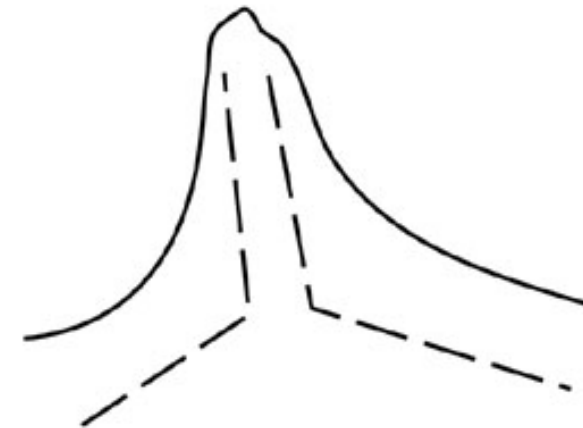
(a) **AULACOGENS**



RRR Triple junction

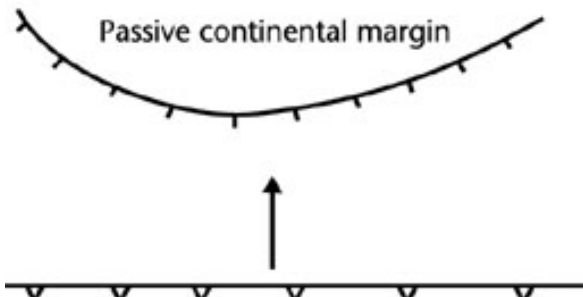


Ocean opening along two successful rift arms



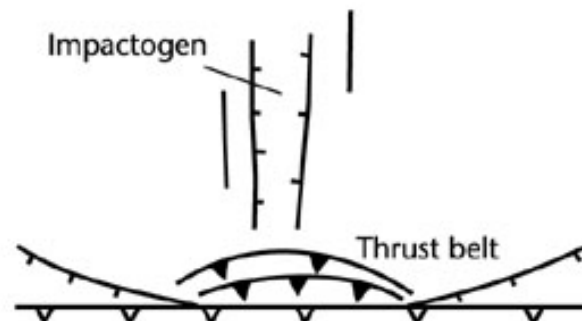
Postrift marine phase

(b) **IMPACTOGENS**



Convergent margin

Precollision phase



Collisional phase

Fig. 3.11 Schematic diagrams to illustrate the development of (a) aulacogens and (b) impactogens, based on Senogr et al. (1978). In (a), successful opening of an ocean basin along two rift arms at a triple junction causes the development of a rift-sag basin along the third, failed rift arm. In (b), collision with a passive continental margin causes an extensional graben at high angles to the orogenic front.

3.3.2 Postrift subsidence at passive continental margin

Synrift subsidence during stretching: Caused by brittle extension of the crust.

Postrift subsidence is driven by:

1. Lithospheric cooling following stretching (the most important factor)
2. Sediment loads
3. Phase change (from gabbro to eclogite) in lower crustal or mantle-lithosphere rocks (not well understood)

Assuming that the bulk of the igneous accretion replaces lithospheric mantle, passive margins with large amounts of magmatic activity should remain relatively elevated compared to non-magmatic margins.

3.3.3 Dynamical models involving lithospheric strength and rheology

A material can only maintain stresses over geological time if the ratio of actual temperature to its melting temperature (known as homologous temperature) is less than about 0.4.

Zone of orogenic thickening are prone to collapse by extension.

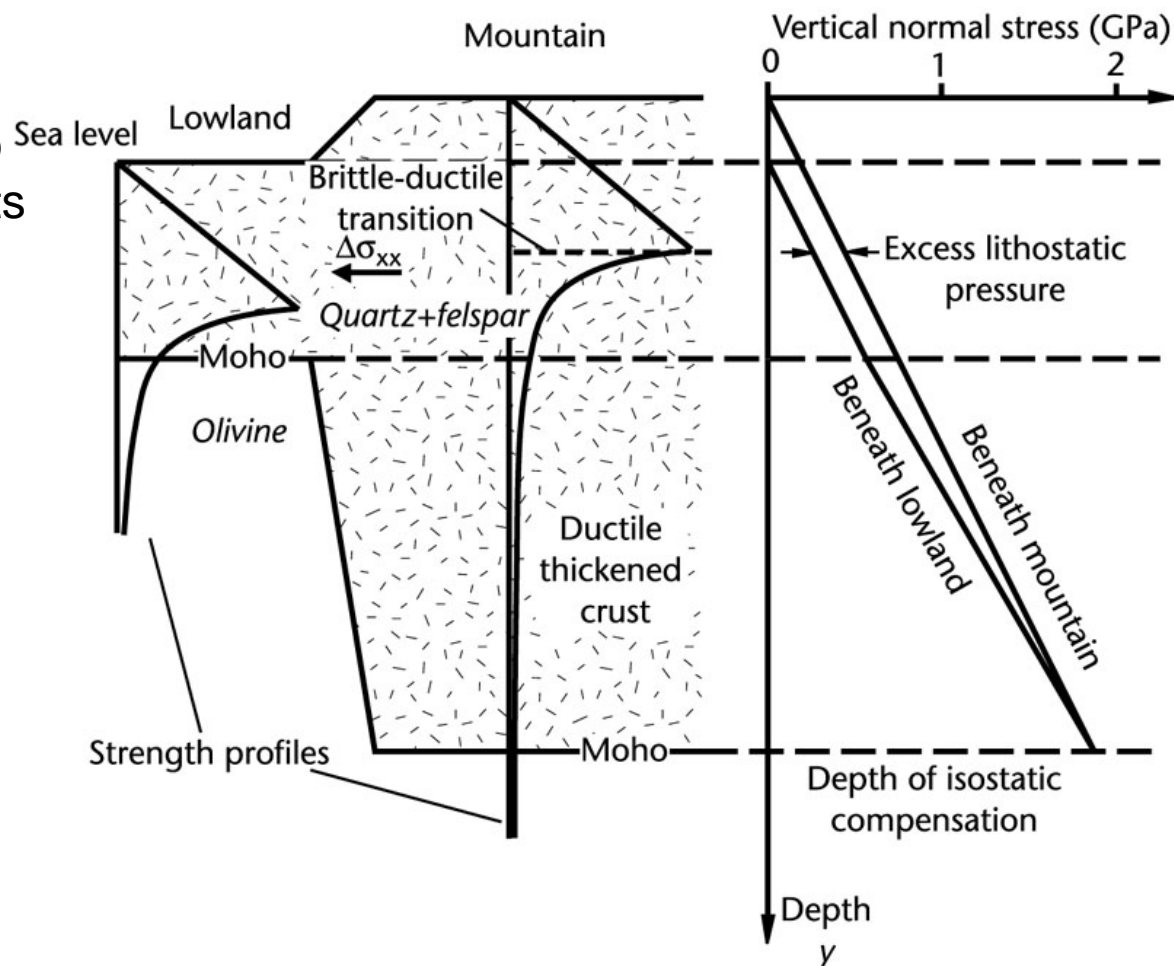


Fig. 3.13 Strength of the continental lithosphere and extensional collapse of thickened continental lithosphere. Thickened crust collapses for two reasons: (i) the quartz-felspar crust is rheologically weak, and (ii) the lithostatic stress is higher under the mountain than under the lowland region, causing it to spread laterally under a horizontal deviatoric stress (130 MPa at 10 km beneath the lowland). If the brittle yield strength of granite is 400 MPa, the brittle-ductile transition should be at a depth of c. 15km beneath the mountain (density

3.4 Uniform stretching of the continental lithosphere

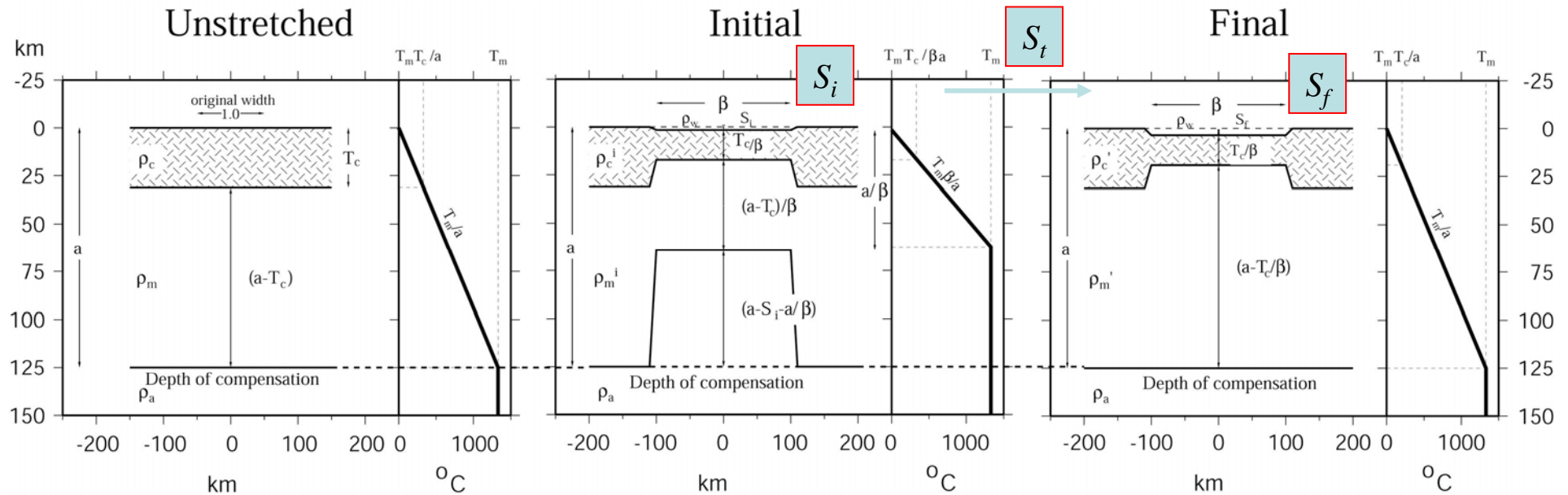
3.4.1 McKenzie's (1978a) uniform stretching model

The total subsidence in an extensional basin is made of two components: an **initial fault controlled subsidence** which is dependent on the initial thickness of the crust and the amount of stretching beta; and a **subsequent thermal subsidence** caused by relaxation of lithospheric isotherms to their pre-stretching position, and which is dependent on the amount of stretching alone.

Whereas the fault-controlled subsidence is modelled as instantaneous, the rate of thermal subsidence decreases exponentially with time. This is the result of a decrease in heatflow with time. The heat flow reaches $1/e$ of its original value after about 50 Myr for a "standard" lithosphere, so at this point after the cessation of rifting, the dependency of the heat flow on beta is insignificant.

3.4 Uniform stretching of the continental lithosphere

3.4.1 McKenzie's (1978a) uniform stretching model



McKenzie's model of extension assumes instantaneous rifting (i.e. duration of rifting = 0) which produces an initial subsidence (S_i) and passive upwelling of hot asthenosphere that results in a thermal perturbation. As this thermal anomaly decays thermal subsidence occurs. If a long time (at least greater than the lithospheric time constant, τ) has elapsed since the rifting such that the thermal perturbation has decayed completely. The final subsidence (S_f) therefore composed of two parts: an initial subsidence, S_i , and a thermal subsidence, S_t .

$$S_f = S_i + S_t$$

S_f is also referred to as

Total amount of Tectonic Subsidence (TTS).

Definitions of parameters

Parameter	Definition	Typical value for oceanic lithosphere
Y_L (or a)	lithospheric thickness	125 km
Y_c (or T_c)	crustal thickness	
ρ_m^* (or ρ_{m0})	mantle density at 0°C	3330 kg m ⁻³
ρ_{sc} (or ρ_m)	average density for subcrustal lithosphere	
ρ_c^* (or ρ_{c0})	crust density at 0°C	2800 kg m ⁻³
ρ_c	average density of the crust	
T_m	temp. at the base of the lithosphere	1333 °C
α_v	coefficient of volume expansion	3.28 x 10 ⁻⁵ °C ⁻¹

Initial subsidence

Pressure at the base of the unstretched lithosphere

The average temperature of the crust: $\frac{T_m T_c}{2a}$

The average temperature of the sub-crustal mantle: $\frac{T_m (T_c + a)}{2a}$

The pressure at the base of the unstretched lithosphere: $\rho_c g T_c + \rho_m g (a - T_c)$

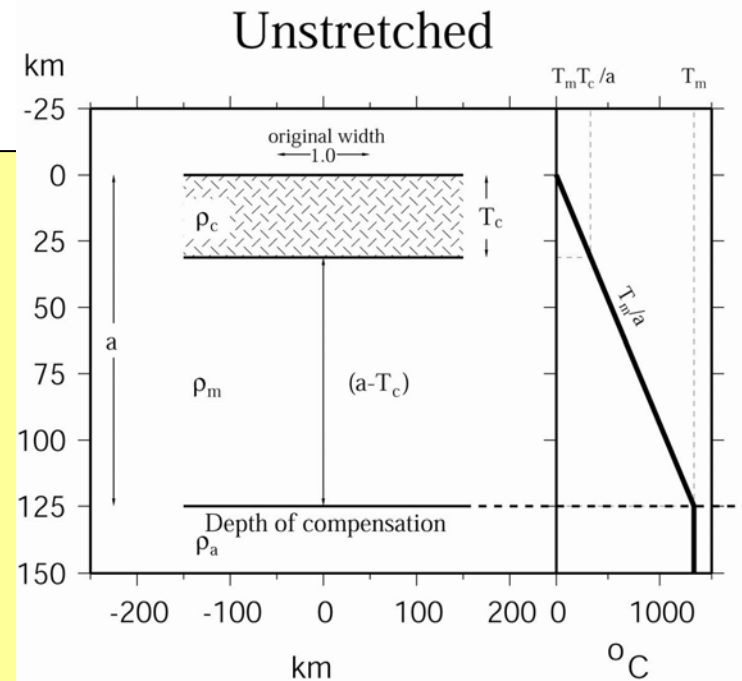
where densities (ρ_c, ρ_m) depends on temperature via the equation of states

$$\rho_c = \rho_{co} \left[1 - \frac{\alpha_v T_m T_c}{2a} \right] \quad \rho_m = \rho_{mo} \left[1 - \frac{\alpha_v T_m (T_c + a)}{2a} \right]$$

where α_v is the volume coefficient of expansion, ρ_{co}, ρ_{mo} are the densities of the crust and mantle at 0°C .

The pressure at the base of the unstretched column becomes:

$$\rho_{co} \left[1 - \frac{\alpha_v T_m T_c}{2a} \right] g T_c + \rho_{mo} \left[1 - \frac{\alpha_v T_m (T_c + a)}{2a} \right] g (a - T_c)$$

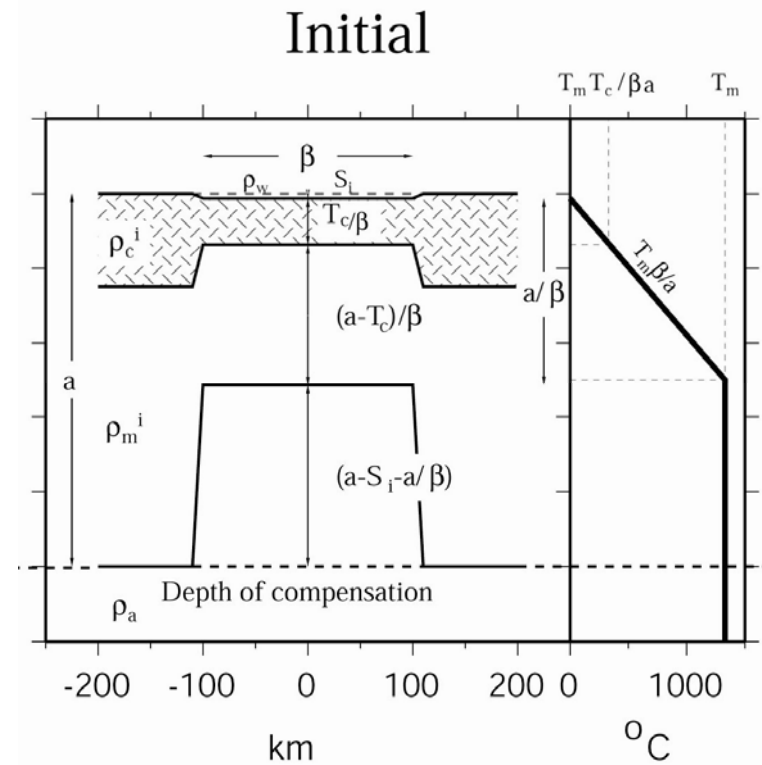


Stretching

Upon stretching each layer moves closer to the surface but its temperature does not change.

Therefore :

- The density at any level in the lithosphere does not change;
- The average density of the lithosphere does not change;
- conservation of mass implies conservation of volume;
- the lithosphere thins by a factor β and the new lithospheric thickness is a/β
- the crust thins by a factor $beta$ and the new crustal thickness : T_c/β
- the thermal gradient is multiplied by β .



Pressure at the base of the stretched lithosphere immediately after rifting

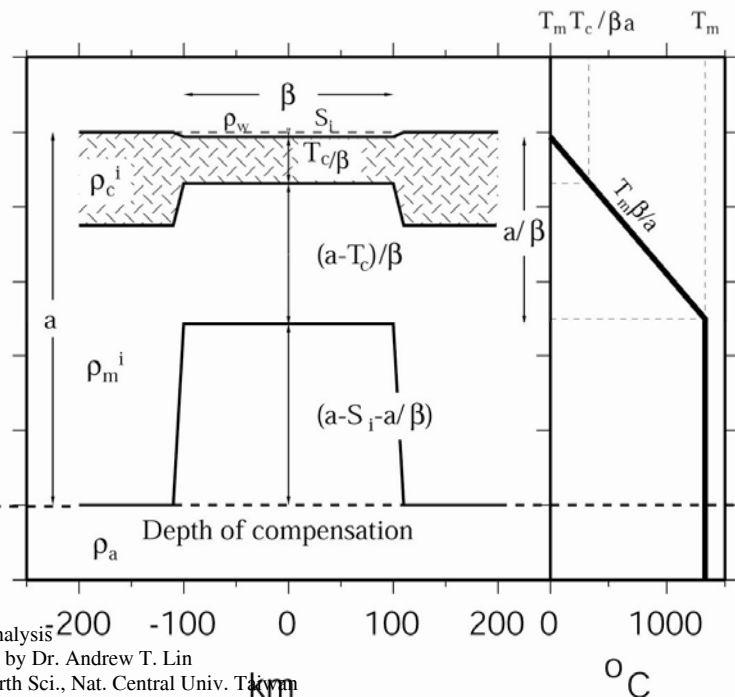
The average temperature of the stretched crust: $\left(\frac{T_m \beta T_c}{a \beta}\right) / 2 = \frac{T_m T_c}{2a}$

The average temperature of the stretched sub-crustal mantle: $\left(\frac{T_m \beta T_c}{a \beta} + T_m\right) / 2 = \frac{T_m (T_c + a)}{2a}$

The pressure at the base of the stretched lithosphere:

$$\rho_w g S_i + \rho_{co} \left[1 - \frac{\alpha_v T_m T_c}{2a} \right] g \frac{T_c}{\beta} + \rho_{mo} \left[1 - \frac{\alpha_v T_m (T_c + a)}{2a} \right] g \left[\frac{a}{\beta} - \frac{T_c}{\beta} \right] + \rho_a g \left[a - S_i - \frac{a}{\beta} \right]$$

Initial



By equating the pressures at the base of the unstretched and stretched lithosphere we get:

Initial subsidence

$$S_i = \frac{a \left\{ (\rho_{mo} - \rho_{co}) \frac{T_c}{a} \left(1 - \frac{\alpha_v T_m T_c}{2a} \right) - \frac{\rho_{mo} \alpha_v T_m}{2} \right\} \left[1 - \frac{1}{\beta} \right]}{[\rho_{mo} (1 - \alpha_v T_m) - \rho_w]}$$

As given on page 80 eq.3.10 of Allen and Allen (2005):

$$Y_s = S_i = \frac{Y_L \left\{ (\rho_m^* - \rho_c^*) \frac{Y_c}{Y_L} \left(1 - \alpha_v \frac{T_m}{2} \frac{Y_c}{Y_L} \right) - \frac{\alpha_v T_m \rho_m^*}{2} \right\} \left[1 - \frac{1}{\beta} \right]}{\left[\rho_m^* (1 - \alpha_v T_m) - \rho_s \right]}$$

For all values of the stretch factor, the initial subsidence S_i is positive (meaning basement subsiding downward) for values of crust/lithosphere thickness ratio of greater than 0.12, corresponding to a crustal thickness Y_c (or T_c) greater than about 15 km within a lithosphere of 125 km (parameter values as given above and sediment density 2000 kgm⁻³).

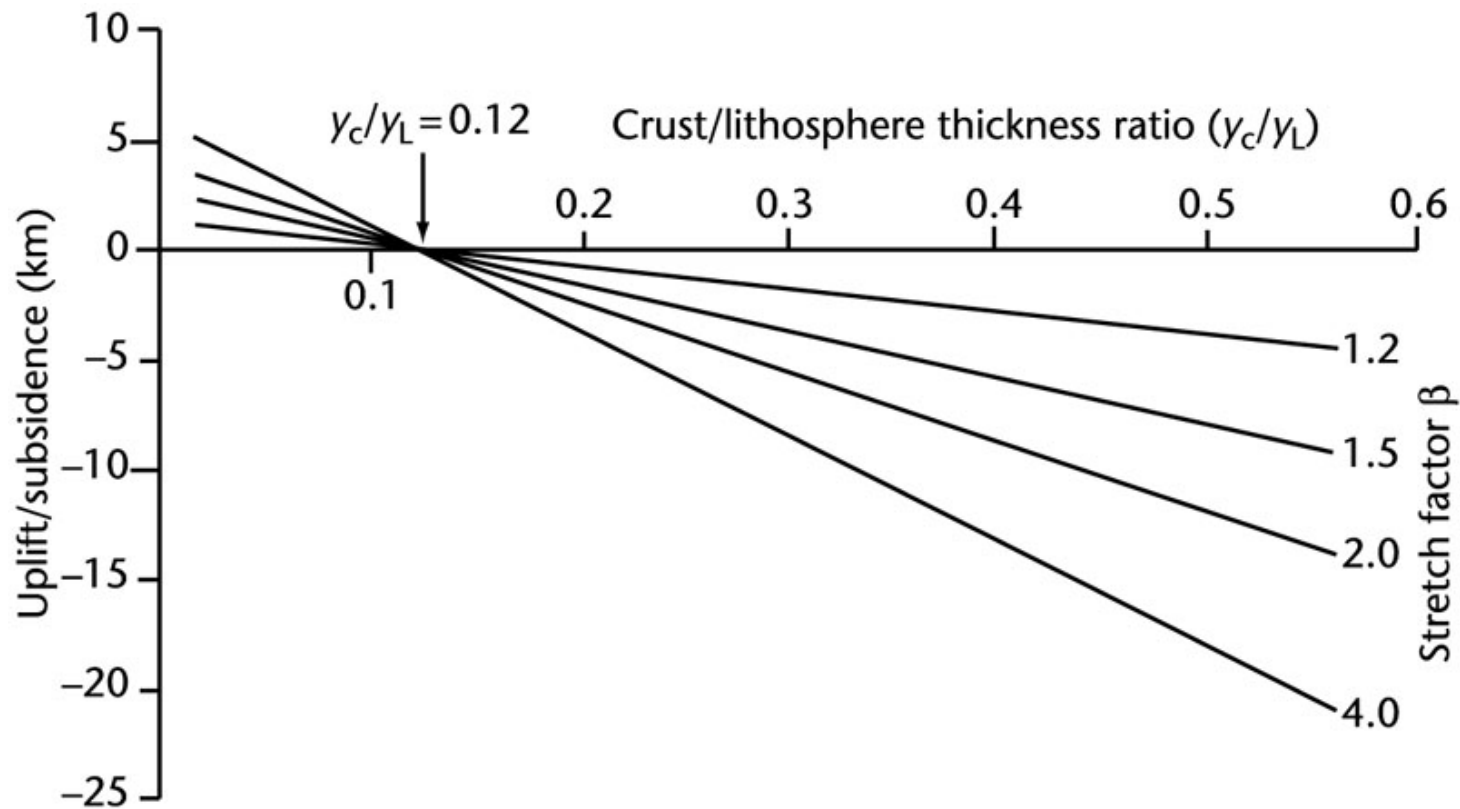


Fig. 3.15 Synrift subsidence as a function of the crustal / lithosphere thickness ratio y_c/y_L for stretch factors β between 1.2 and 4, using the uniform stretching model. Crustal, mantle and sediment densities are 2700 kgm^{-3} , 3300 kgm^{-3} and 2000 kgm^{-3} respectively. At a crust/lithosphere thickness ratio of 0.12 (corresponding to a crust of 15km in a lithosphere 125 km thick), there is neither uplift nor subsidence during rifting. For thinner crusts, uplift occurs, and for thicker crusts, subsidence occurs. Since crustal thicknesses are typically 30-35km, the synrift phase should be characterized by subsidence.

Variations of initial subsidence with beta and potential temperature

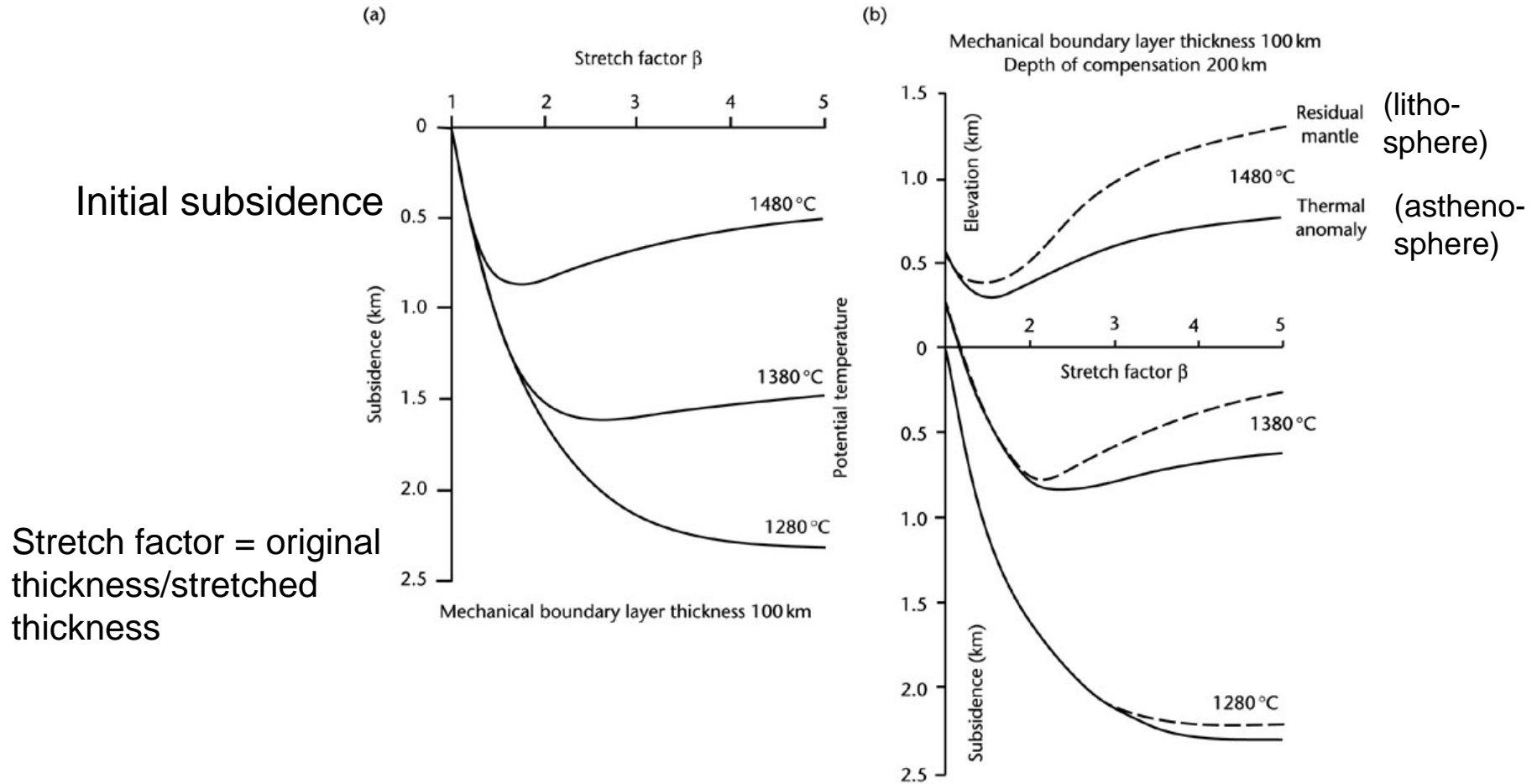


Fig. 3.12 Uplift and subsidence associated with plume activity at a spreading margin (after White and McKenzie 1989). (a) Subsidence at the time of rifting as a function of the stretch factor for potential temperatures of 1280°C, and 1480°C. Each curve incorporates the effects of lithospheric thinning, and crustal additions of melts caused by decompression of the mantle; (b) The effects of the reduced density of the abnormally hot asthenosphere (thermal anomaly) and the reduced density of the depleted lithosphere to be elevated well above the level expected for an asthenosphere of normal temperature. The depth of compensation of 200km is typical of the depth over which anomalously hot mantle is likely to extend.

$$q = \frac{KT_m}{Y_L} \left\{ 1 + \frac{2\beta}{\pi} \sin\left(\frac{\pi}{\beta}\right) e^{\left(-\frac{t}{\tau}\right)} \right\}$$

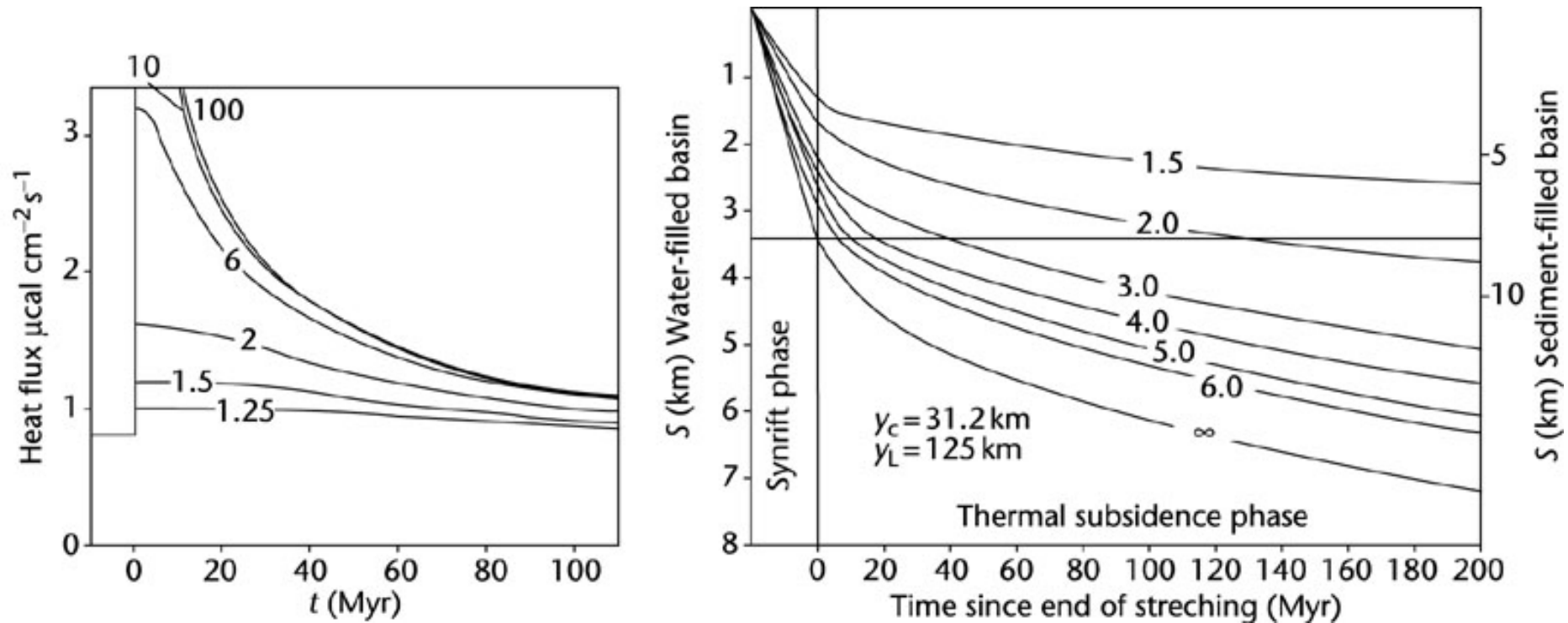


Fig. 3.16 Heat flow and subsidence as a function of the stretch factor using the uniform stretching model. (a) Heat flux against time (after McKenzie 1987a, p.28). After c. 50Myr, the heat fluxes are similar for all values of stretch factor; (b) Elevation change (subsidence) against time for water-filled basins, showing the negative exponential form of the subsidence history during the postrift, thermal contraction phase (after Sclater et al. 1980a).

```

% Exercise 3_1, Basin analysis
% McKenzie model
% Sonia Scarselli ETH-Zurich, sonia.scarselli@erdw.ethz.ch
%This program calculates the syn-rift subsidence, the thermal (postrift)
subsidence and the total subsidence, ...
...and plots the total subsidence as a function of time.
% The initial parameters can be changed to evaluate different synrift
subsidence and thermal subsidence
% curve

```

```
clear;
```

```
% Define initial parameters
```

```

y_c    = 35000;    % Initial crustal thickness in m           [m]
y_l    = 125000;   % Initial lithospheric thickness in m        [m]
rho_m0 = 3330;    % Density of the mantle at 0 degrees celcius [kg/m^3]
rho_c0 = 2800;    % Density of the crust at 0 degrees celcius [kg/m^3]
rho_s   = 2066;   % Density of sediments                    [kg/m^3]
alpha_v = 3.28e-5; % volumetric coefficient of thermal expansion [1/K]
Tm      = 1333;   % Temperature of the mantle                [C]
kappa   = 1e-6;   % Thermal diffusivity                    [m^2/s]
time_my = 0:150;  % Time                                    [my]
time_s  = time_my*365*24*3600*1e6; % Time in seconds
beta    = 3;      % stretch factor

```

```
% Step 1: Calculate synrift subsidence
```

```

ys =
y_l*((rho_m0-rho_c0)*y_c/y_l*(1-alpha_v*Tm*y_c/y_l)-alpha_v*Tm*rho_m0/2)*(1-
1/beta)/(rho_m0*(1-alpha_v*Tm)-rho_s)

```

```
% Step 2: Calculate thermal subsidence with time
```

```

E0 = 4*y_l*rho_m0*alpha_v*Tm/(pi^2*(rho_m0-rho_s));
tau = y_l^2/(pi^2*kappa);

```

```
S = E0*beta/pi*sin(pi/beta)*(1-exp(-time_s/tau));
```

```
% Calculate total subsidence
```

```

S_total = ys + S; %Total subsidence in meters
S_thermal = S; %Thermal subsidence in meters

```

```

S_total = S_total /1e3; %Total subsidence in km's
S_thermal = S_thermal/1e3; %Thermal subsidence in km's

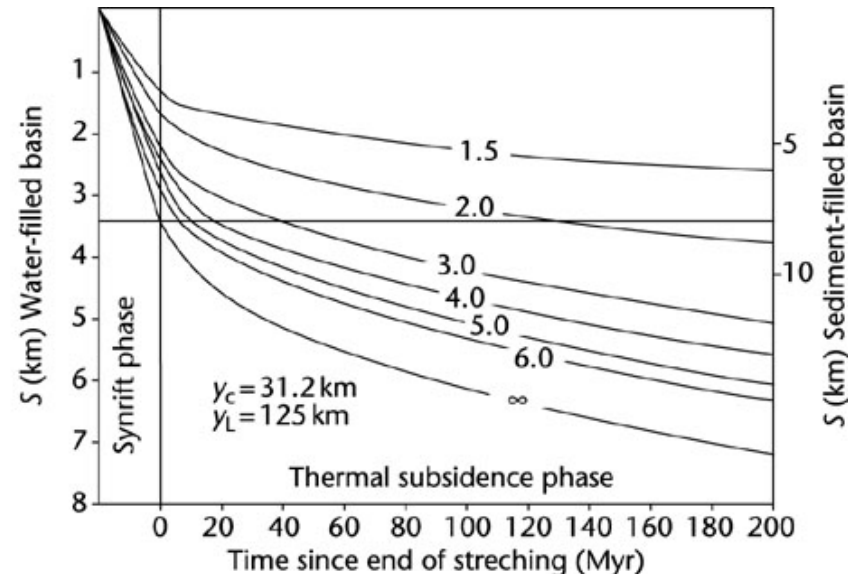
```

```
% Plotting
```

```

plot(time_my,S_total,'r-')
title('Synrift and thermal subsidence, part a')
xlabel('Time since end of rifting [My]')
ylabel('Thermal subsidence [km]');
legend(num2str(beta))
grid on

```



3.4.2 Uniform stretching at passive continental margins

Final subsidence (S_f , or Total Tectonic Subsidence, TTS)

As the thermal perturbation decays completely final subsidence can be obtained by balancing the pressure at the base of the unstretched column with the final column.

The pressure at the base of the final column is given by $\rho_w S_f g + \rho_c' \frac{T_c}{\beta} g + \rho_m' \left[a - S_f - \frac{T_c}{\beta} \right] g$

where ρ_c' , ρ_m' are the densities of the cooled and stretched crust and sub-crustal mantle respectively.

The average temperature of the cooled, stretched crust:

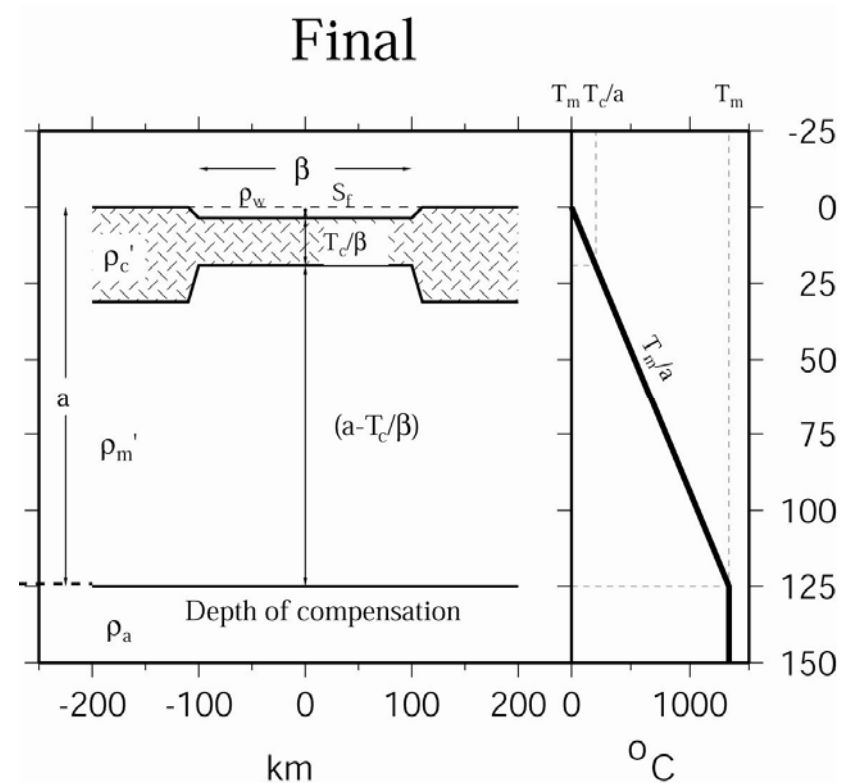
$$\left(\frac{T_m}{a} \frac{T_c}{\beta} \right) / 2 = \frac{T_m T_c}{2\beta a}$$

The average temperature of the cooled, stretched sub-crustal mantle:

$$\left(\frac{T_m}{a} \frac{T_c}{\beta} + T_m \right) / 2 = \frac{T_m}{2} \left(1 + \frac{T_c}{\beta a} \right)$$

Therefore

$$\rho_c' = \rho_{co} \left(1 - \frac{\alpha_v T_m T_c}{2\beta a} \right) \quad \rho_m' = \rho_{mo} \left(1 - \frac{\alpha_v T_m T_c}{2\beta a} - \frac{\alpha_v T_m}{2} \right)$$



Equating the pressures at the base of the unstretched and final columns gives

$$S_f = \frac{a(\rho_m' - \rho_m) + T_c \left(\rho_m + \frac{\rho_c'}{\beta} - \frac{\rho_m'}{\beta} - \rho_c \right)}{(\rho_m' - \rho_w)}$$

Using the parameters listed before, we get

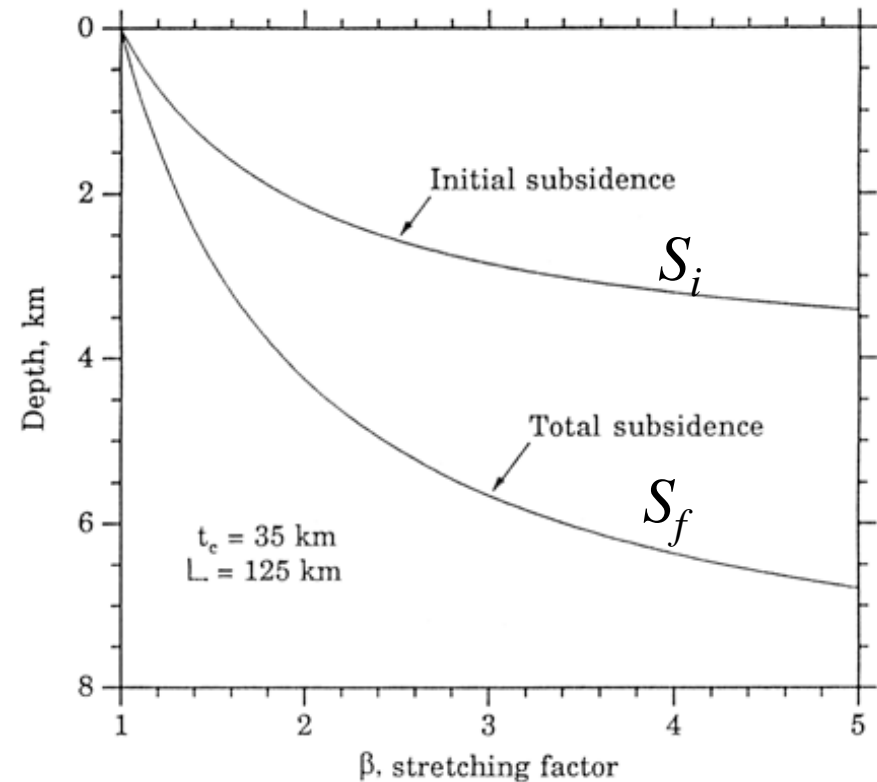
$$\rho_c' = 2795 \text{ kg m}^{-3}$$

$$\rho_m' = 3251 \text{ kg m}^{-3}$$

$$S_f = 4.927 \text{ km}$$

Therefore, the density of the crust and lithosphere increases from the initial conditions and the lithosphere subsides.

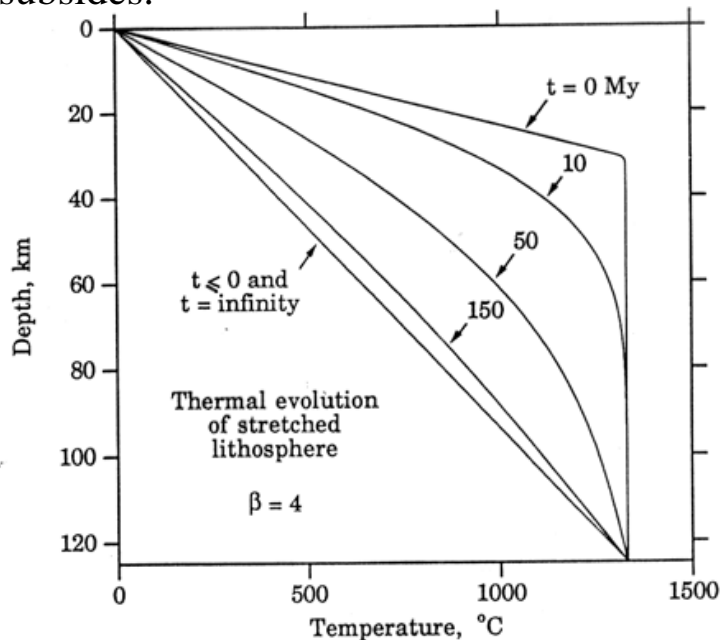
Initial (S_i) and total subsidence (S_f) as a function of β . Thickness of crust and the lithosphere is 35 km and 125 km respectively (Angevine et al., 1990).



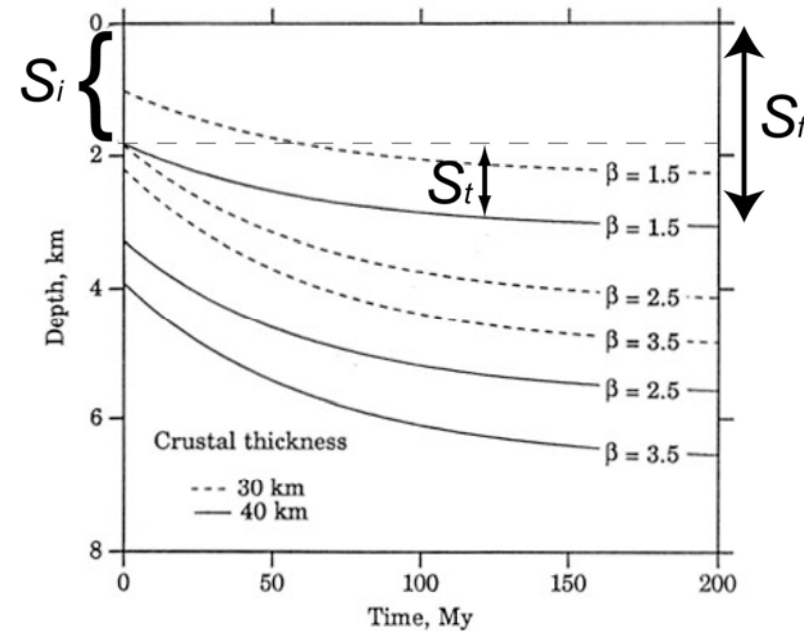
Thermal subsidence (S_t)

Above calculations on S_i and S_f are two “end-member” points: S_i corresponding to the onset of rifting and the other after a long time has elapsed since rifting.

After stretching, the lithosphere is warmer than it was initially; it will progressively cool down until the geothermal gradient is the same as it was initially. As lithosphere cools it subsides.



Cooling of the lithosphere following rifting; assumed thickness for the lithosphere is 125 km and β is 4.



For intermediate times since rifting, thermal perturbations remain and the **full thermal treatment** of the problem must be considered.

Using one-dimensional heat flow equation the temperature T at a time t since rifting in the stretched lithosphere is given by (McKenzie, 1978)

$$T = T_m \left(1 - \frac{z}{a} \right) + \frac{2T_m}{\pi} \sum_{n=1}^{\infty} \frac{(-1)^{n+1}}{n} \left[\frac{\beta}{n\pi} \sin \frac{n\pi}{\beta} \right] e^{(-n^2 t / \tau)} \sin \frac{n\pi z}{a}$$

where z is the coordinate in the direction in which heat flow occurs. It is often sufficient to truncate the solution at $n = 1$ since the contributions from terms for $n > 1$ are small because of the e^{-n^2} dependence in the summation.

$$T = T_m \left(1 - \frac{z}{a} \right) + \frac{2T_m}{\pi} \left[\frac{\beta}{\pi} \sin \frac{\pi}{\beta} \right] e^{(-t/\tau)} \sin \frac{\pi z}{a}$$

The thermal subsidence, $S_t(t)$, as a result of this cooling is determined by isostatic balance with a column of unstretched lithosphere. The elevation, $e(t)$, above the final depth to which the surface of the crust sinks is given:

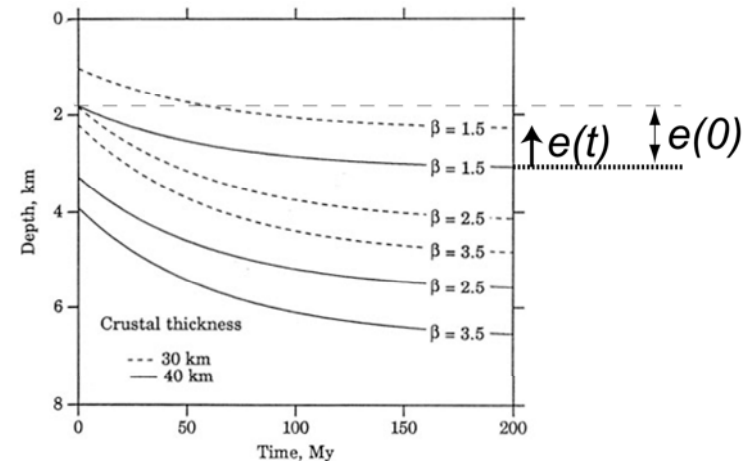
$$e(t) = E_0 r e^{-t/\tau}$$

where

$$E_0 = \frac{4a\rho_{mo}\alpha_v T_m}{\pi^2(\rho_{mo} - \rho_w)} \quad r = \left(\frac{\beta}{\pi} \right) \sin \frac{\pi}{\beta}$$

τ is the lithospheric time constant and is given by $\tau = \frac{a^2}{\pi^2 \kappa}$

It measures how quickly the lithosphere goes back to thermal equilibrium by conduction.



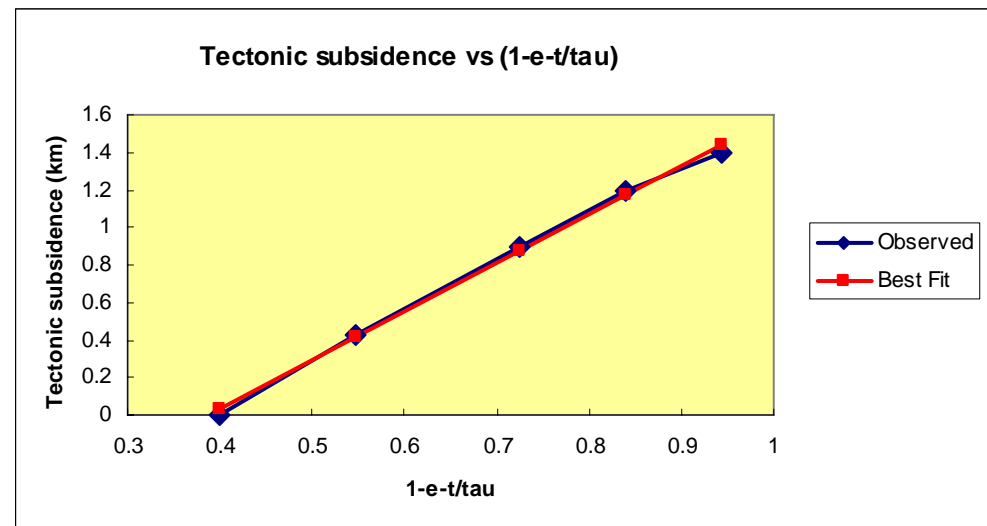
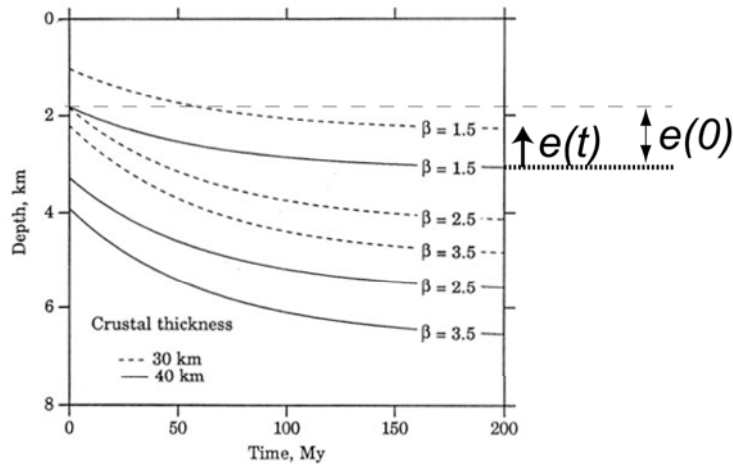
The thermal subsidence, $S_t(t)$, since rifting: $S_t(t) = e(0) - e(t)$

where $e(0)$ is the elevation at $t=0$. $e(0)=E_0r$, therefore

$$S_t(t) = E_0r(1 - e^{-t/\tau})$$

A plot of S_t versus $(1-e^{-t/\tau})$ will have a slope E_0r . This function depends on β , the amount of extension.

β stretching factor can be determined from the slope (E_0r) of the S_t vs. $(1-e^{-t/\tau})$ plot.



```

%Exercise 3_2, Basin analysis
%% Evaluation of beta
% Sonia Scarselli, ETH-Zurich, sonia.scarselli@erdw.ethz.ch
% Calculation of the Stretch Factor from Thermal Subsidence Data
% This program calculates the stretch factor that best fits the thermal
% subsidence data
...derived from a decompaction and backstripping analysis of a borehole or
surface
...stratigraphic section.

```

```
clear;
```

```
% Define some initial parameters
```

```

y_c      = 35000;           % Initial crustal thickness in m
[m]
y_l      = 125000;         % Initial lithospheric thickness in m
[m]
rho_m0   = 3330;           % Density of the mantle at 0 degrees
celcius  [kg/m^3]
rho_c0   = 2800;           % Density of the crust at 0 degrees
celcius  [kg/m^3]
rho_s    = 1000;           % Density of the infilling material
[kg/m^3]
alpha_v  = 3.28e-5;        % Thermal expansivity
[1/K]
Tm       = 1333;           % Temperature of the mantle
[C]
kappa    = 1e-6;           % Thermal diffusivity
[m^2/s]
time_my  = [0, 55, 65, 100]; % Time since end of rifting
[my]
time_s   = time_my*365*24*3600*1e6; % Time since end of rifting in seconds
sub      = [-.217 1.031 1.251 1.854]; % Subsidence in km

```

```

tau      = y_l^2/(pi^2*kappa);
E0       = 4*y_l*rho_m0*alpha_v*Tm/(pi^2*(rho_m0-rho_s));

```

```

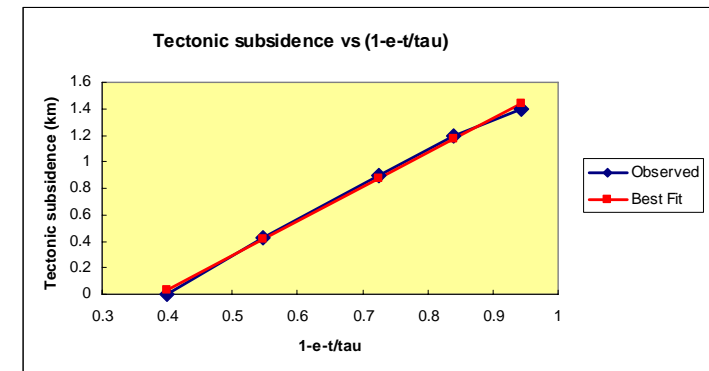
x        = ((1-exp(-time_s/tau))); %X-axis
y        = sub*1000;               %Y-axis

```

```

plot(x,y,'o-r')                    %Plot the data points
xlabel('1-exp(-t/\tau)')
ylabel('Thermal subsidence [m]')

```



```

% Calculate the best-fit through the data points by using the fitting tool
of matlab (see the figure window -> Tools -> basic fitting)
%  $y = p1*x + p2$  -> best fit gives  $p1 = 2218.6$  (slope)

slope_bestfit = 2218.6;

% We know that the slope of the best-fit line through the points is given by
the formula
...slope =  $E0*(beta/pi)*sin(pi/beta)$ . We know  $E0$  and need to find  $beta$ .

% Two methods are provided to calculate the stretch factor. The first is
simply by manual trial and error,
...where you keep modifying your estimate of the stretch factor until the
linear best fit slope is correct.

% The second approach is doing this with a computer. This is called
iterations and is shown below.

% Approach 1, do it by hand
beta = .2;
slope =  $E0*beta/pi*sin(pi/beta)$  %if slope is not equal to slope_bestfit,
modify beta

% Approach 2, let the computer do the work
beta = 1;
dbeta = .1;
iteration_error = 1;
while abs(iteration_error) > 1e-10 %do it until the difference between
the best-fitted slope and the calculated slope is smaller than 1e-10

    slope =  $E0*beta/pi*sin(pi/beta)$ ;
    iteration_error = slope-slope_bestfit;

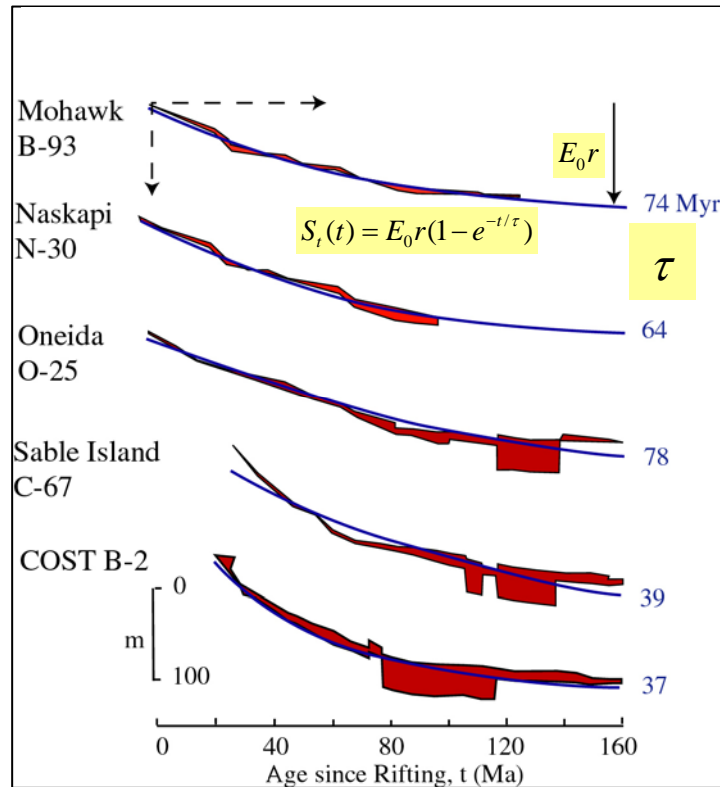
    if iteration_error<0
        beta = beta + dbeta;
    else
        dbeta = dbeta/2;
        beta = beta-dbeta;
    end

end
beta

```

The exponential nature of rift-type basin backstrip curves

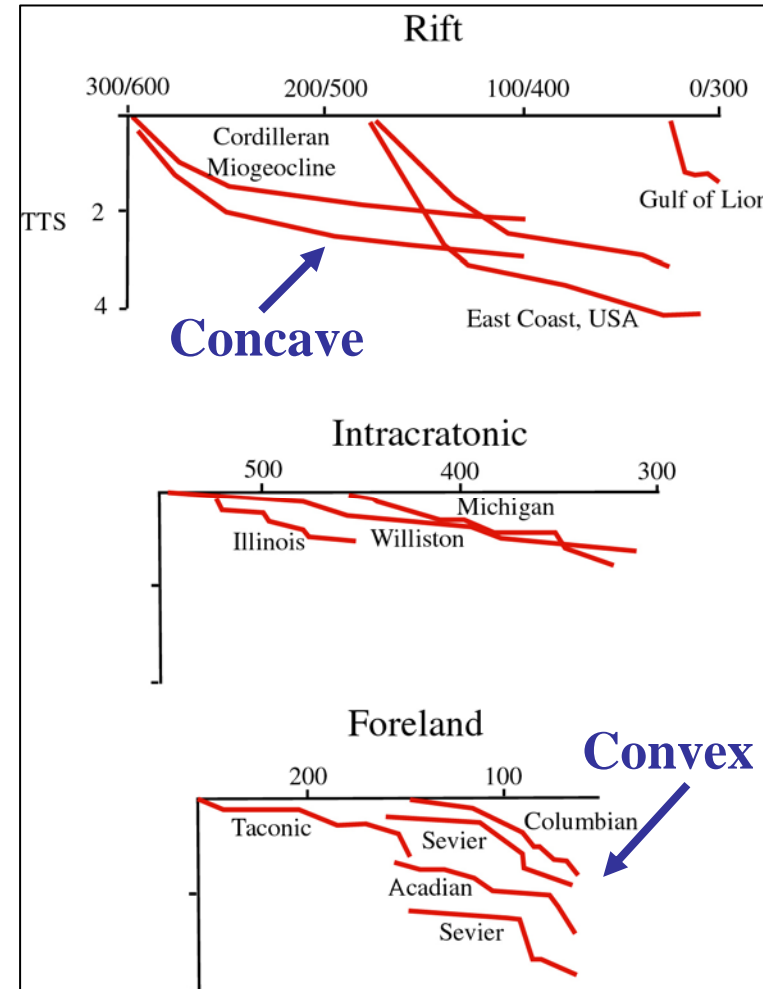
Backstripping studies of well data along the **East Coast, USA and Canada Passive Margin** clearly show the exponential nature of rift-type basin tectonic subsidence curves



The numbers to the right of each backstrip is the best fit exponential decay term, τ . [τ is the value of t when $S_i(t) = E_0 r (1 - e^{-1})$, or $S_i(t) = E_0 r * 0.632$.]

Higher τ subsidence slower; lower τ subsidence faster

Backstrip curves for **Rift-type basins** are generally concave.



Curves for **Foreland-type basins**, in contrast, are generally convex.

Example plots of S_t vs. $(1-e^{-t/\tau})$ for the COST B-2 well.

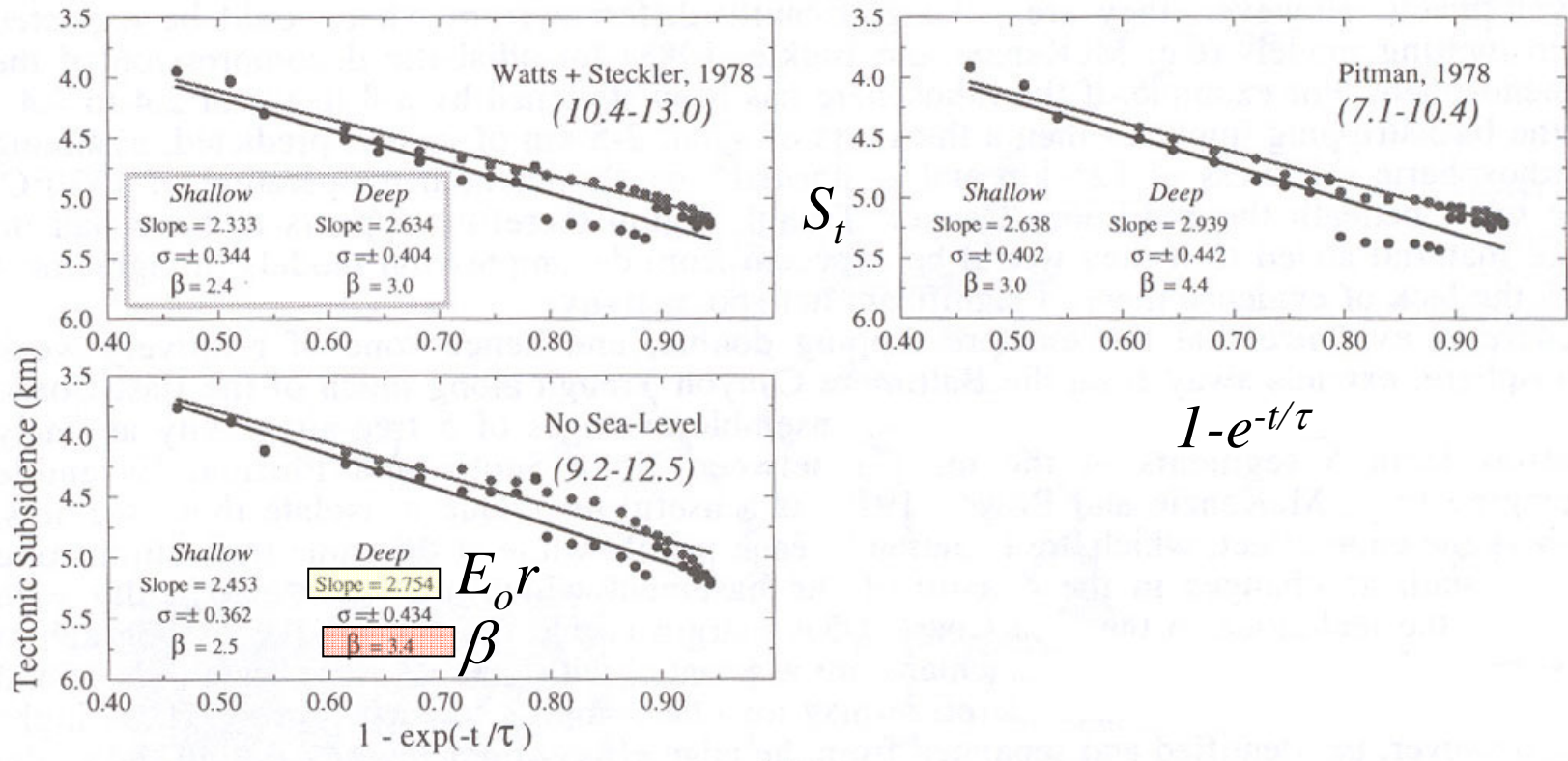


Fig. 9 Plot of tectonic subsidence vs. $(1-e^{-t/\tau})$ for the COST B-2 well. τ = thermal time constant = 62.5 Ma, t = age (Ma) since rifting. The tectonic subsidence curves have been calculated for different assumptions concerning the water depth of deposition and sea-level changes through time. Heavy dots = shallow water depth. Grey dots = deep water depth. Sea-level curves are based (Pitman, 1978) (right panel) and (Watts and Steckler, 1979) (upper left panel). The lower left panel shows the tectonic subsidence for no sea-level change. β = stretching factor. σ = standard deviation (km) between the tectonic subsidence and the best fit straight line. The numbers in brackets in the upper right of each panel indicate the range of thickness of the stretched crust based on the best fit estimates of β .

3.5 Modifications to the uniform stretching model

Assumptions in the uniform stretching model:

1. Stretching is uniform with depth;
2. Stretching is instantaneous;
3. Stretching is by pure shear;
4. The necking depth is zero;
5. Airy isostasy is assumed to operate throughout;
6. There is no radiogenic heat production;
7. Heat flow is in one dimension (vertically) by conduction;
8. There is no magmatic activity;
9. The asthenosphere has a uniform temperature at the base of the lithosphere.

Modifications to uniform stretching models

- ◆ **Nonuniform (depth-dependent) stretching**: the mantle lithosphere may stretch by a different amount to the crust;
- ◆ **Pure versus simple shear**: the lithosphere may extend along trans-crustal or trans-lithospheric detachments by simple shear.
- ◆ **Protracted rifting**: continental rifts typically have synrift phases lasting 20-30 Myr.
- ◆ **Elevated asthenospheric temperatures**: the base of the lithosphere may be strongly variable in its temperature structure due to the presence of convection systems such as hot plumes.
- ◆ **Magmatic activity**: the intrusion of melts at high values of stretching modifies the heat flow history and thermal subsidence at passive margins.
- ◆ **Induced mantle convection**: the stretching of the lithosphere may induce secondary mantle convection in the region of upwelled asthenosphere.
- ◆ **Radiogenic heat production**: the granitic crust provides an additional important source of heat.
- ◆ **Depth of necking**: necking may be centered on strong layers deeper in the midcrust or upper mantle lithosphere.
- ◆ **Flexural compensation**: the continental lithosphere has a finite elastic strength, and flexural rigidity, particularly in the postrift thermal subsidence phase.

3.5.1 Nonuniform (depth-dependent) stretching: Two models (discontinuous vs. continuous)

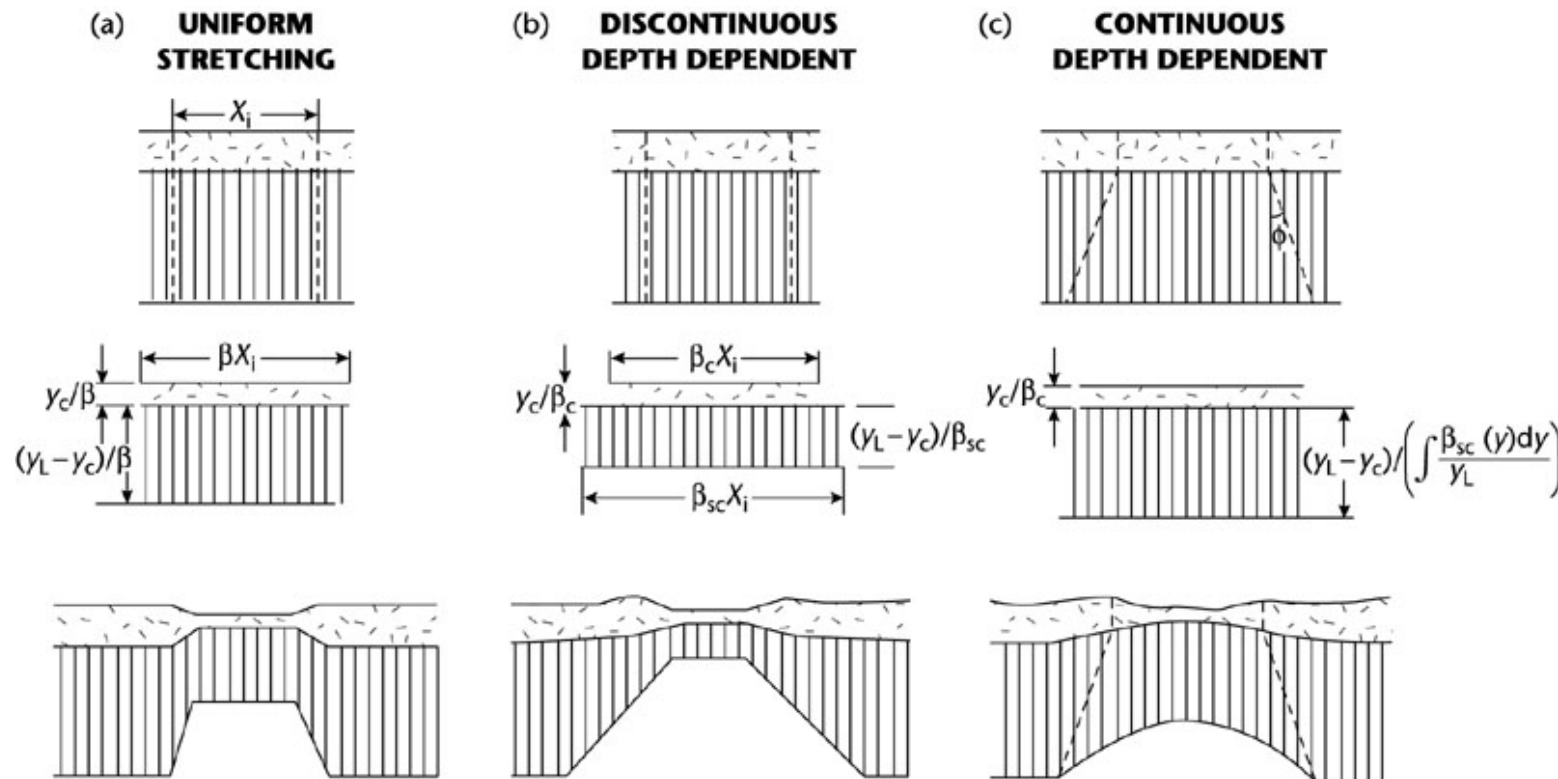


Fig. 3.18 Schematic diagrams to illustrate differences between (a) uniform, (b) discontinuous, and (c) continuous depth-dependent stretching. (a) Uniform extension in which the crust and subcrustal lithosphere extend by identical amounts; (b) Discontinuous depth-dependent extension in which the crust extends by a different amount to the subcrustal lithosphere, necessitating a decoupling between the two layers. The crustal and subcrustal extensions are independent but are uniform throughout the crust and subcrustal lithosphere; (c) Continuous depth-dependent extension in which the stretching is a continuous function of depth in the subcrustal lithosphere and the crustal stretching is the same as in (a) and (b).

Basin Analysis
 Prepared by Dr. Andrew T. Lin,
 Dept. Earth Science, National Central University

Both sets of models make a first-order prediction – that zones of continental stretching should be characterized by **elevated rift margin topography**.

Roles of rheology during rifting, an example from the Iberia margin

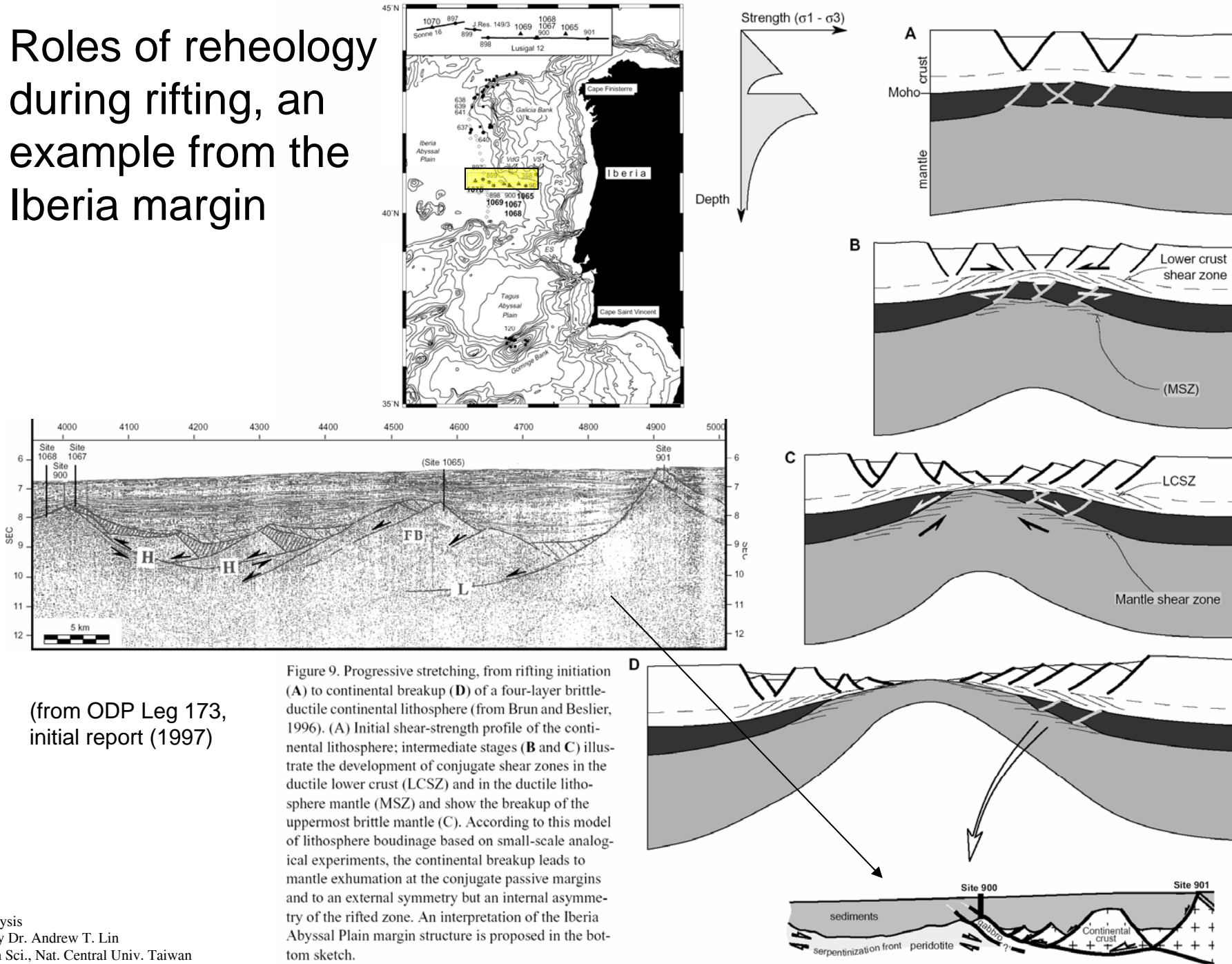
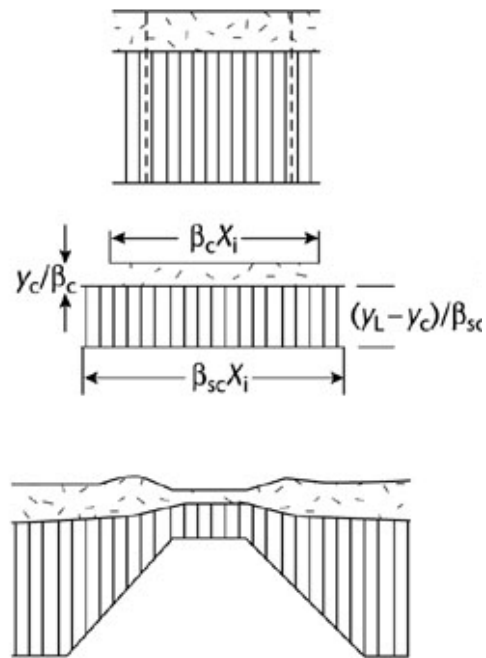


Figure 9. Progressive stretching, from rifting initiation (A) to continental breakup (D) of a four-layer brittle-ductile continental lithosphere (from Brun and Beslier, 1996). (A) Initial shear-strength profile of the continental lithosphere; intermediate stages (B and C) illustrate the development of conjugate shear zones in the ductile lower crust (LCSZ) and in the ductile lithosphere mantle (MSZ) and show the breakup of the uppermost brittle mantle (C). According to this model of lithosphere boudinage based on small-scale analogical experiments, the continental breakup leads to mantle exhumation at the conjugate passive margins and to an external symmetry but an internal asymmetry of the rifted zone. An interpretation of the Iberia Abyssal Plain margin structure is proposed in the bottom sketch.

(from ODP Leg 173, initial report (1997))

Discontinuous stretching with depth

(b) **DISCONTINUOUS
DEPTH DEPENDENT**



If the lower zone stretches by ductile deformation more than the brittle upper zone, uplift should occur if the depth to decoupling approximates the crustal thickness ($d \sim \gamma_c$). This uplift occurs at the same time as extension.

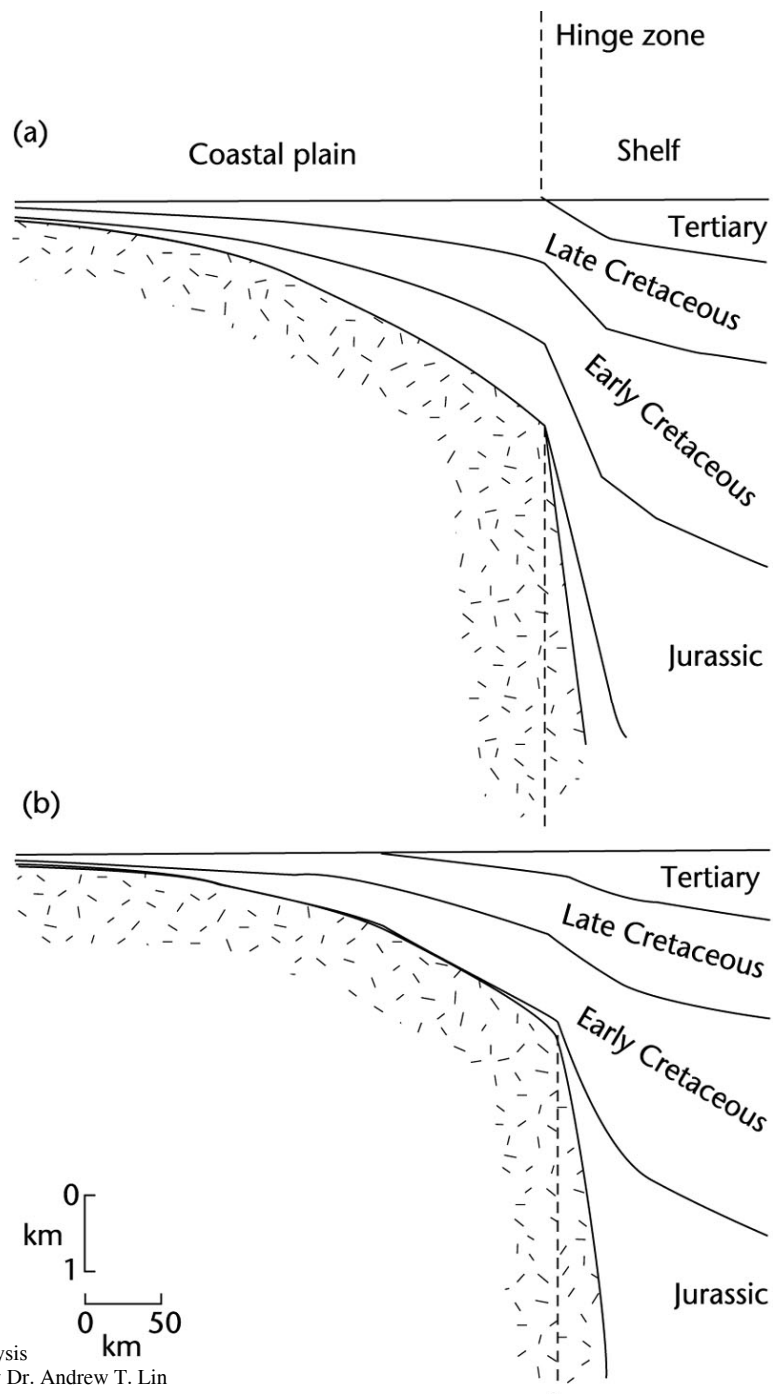


Fig. 3.19 Synthetic stratigraphy along profiles crossing the coastal plain and shelf off New Jersey constructed using the flexural loading model of Watts and Thorne (1984). (a) **One-layer uniform stretching model**; (b) **two-layer model in which the lithosphere and crust are thinned by equal amounts seaward of the hinge zone, but only the mantle lithosphere is thinned landward of the hinge zone.** The lithospheric thinning promotes early uplift of the zone landward of the hinge line, and helps to explain the absence of Jurassic strata from this region (after Steckler et al. 1988).

One layer model (a) over-predicts synrift sediment thickness (Jurassic) beneath the coastal plain. Two-layer model (b) explains the lack of synrift (Jurassic) stratigraphy by the lateral loss of heat to the flanks of the rift, causing uplift and subaerial emergence.

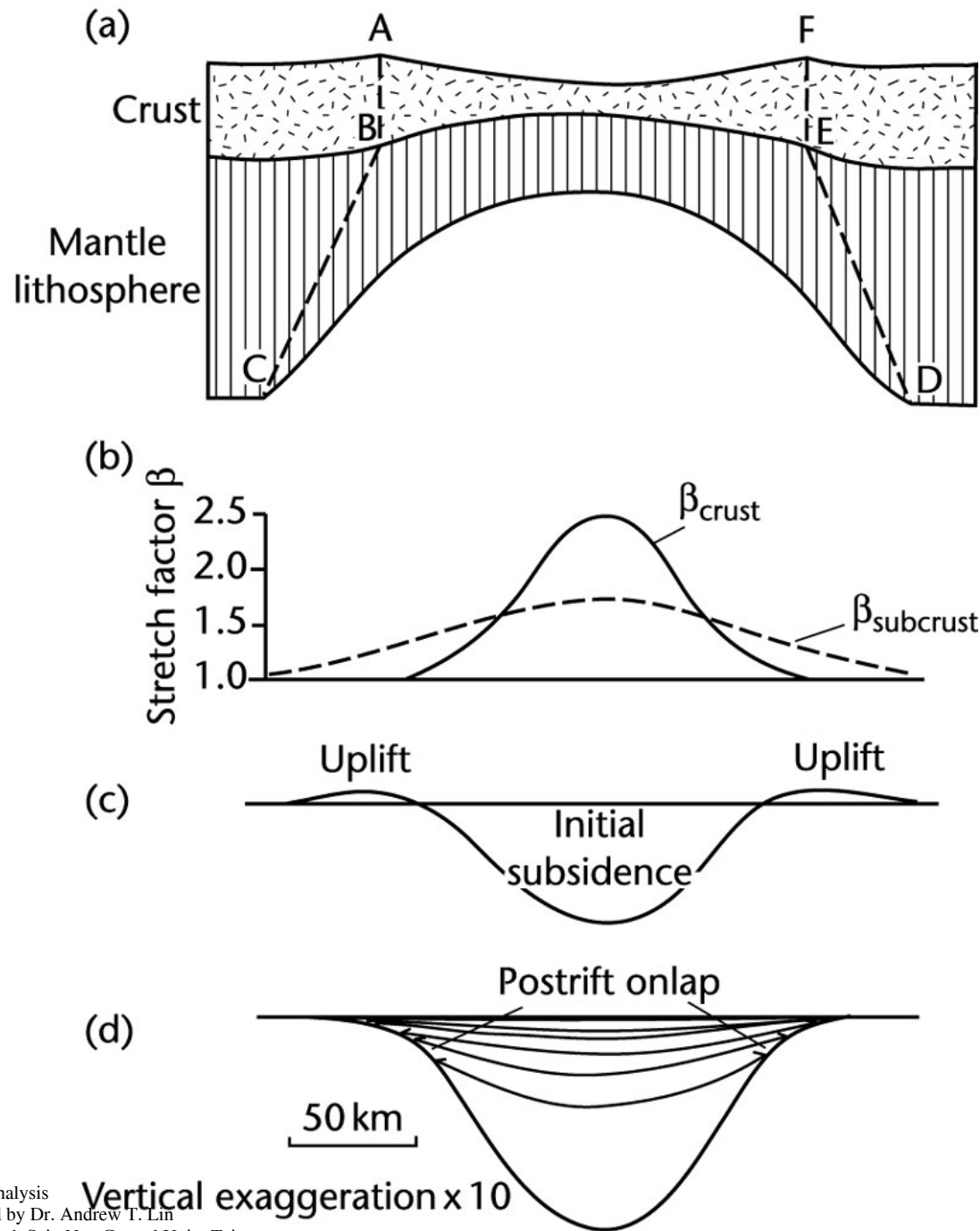
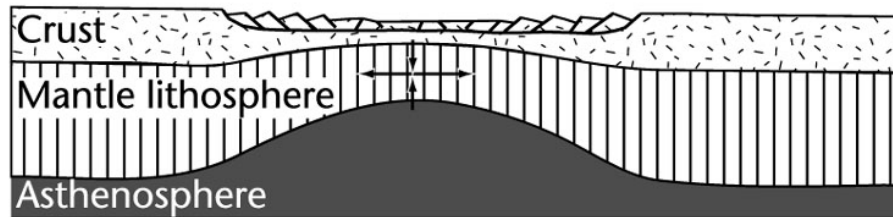


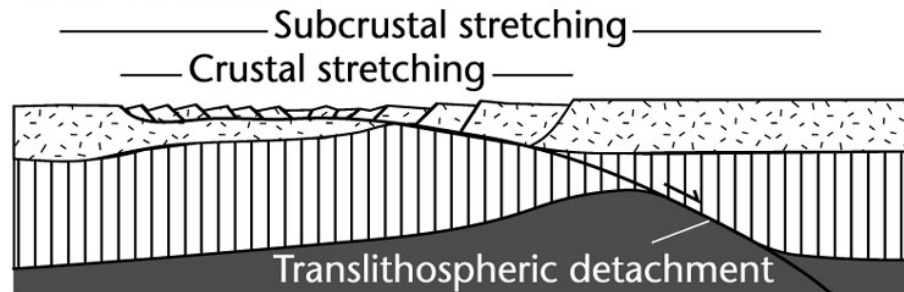
Fig. 3.20 Basin filling pattern resulting from **continuous depth-dependent stretching** (Rowley and Sahagian 1986; White and McKenzie 1988). (a) Geometry of a tapering region of extension in the subcrustal lithosphere; (b) Stretch factors in the crust and subcrustal lithosphere as a function of horizontal distance (c) Initial subsidence and uplift immediately after stretching, showing prominent rift flank uplift; (d) Total subsidence 150 Myr after rifting, showing progressive onlap of the basin margin during the thermal subsidence phase, giving a "steer's head" geometry.

3.5.2 Pure versus simple shear

(a) **PURE SHEAR**



(b) **SIMPLE SHEAR**



(c) **SIMPLE SHEAR-PURE SHEAR**

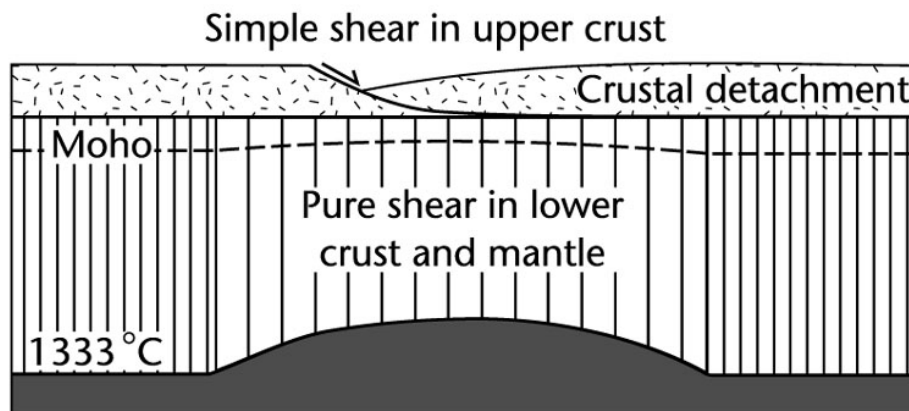


Fig. 3.21 Models of strain geometry in rifts (Coward 1986; Buck et al. 1988). (a) Pure shear geometry with an upper brittle layer overlying a lower ductile layer, producing a symmetrical lithospheric cross-section with the initial fault-controlled subsidence spatially superimposed on the thermal subsidence. The ductile stretching may be accompanied by dilation due to the intrusion of melts (Royden et al. 1980); (b) Simple shear geometry with a through-going low-angle detachment dividing the lithosphere into an upper plate or hangingwall, and a lower plate or footwall. Thinning of the lower lithosphere is relayed along the detachment plane, producing a highly asymmetrical lithospheric cross-section (after Wernicke 1981, 1985). Initial fault-controlled subsidence is spatially separated from the thermal subsidence; (c) Hybrid model of simple shear in the upper crust on listric (shown) or planar faults, and pure shear in the ductile lower crust and mantle lithosphere (Kusznir et al. 1991).

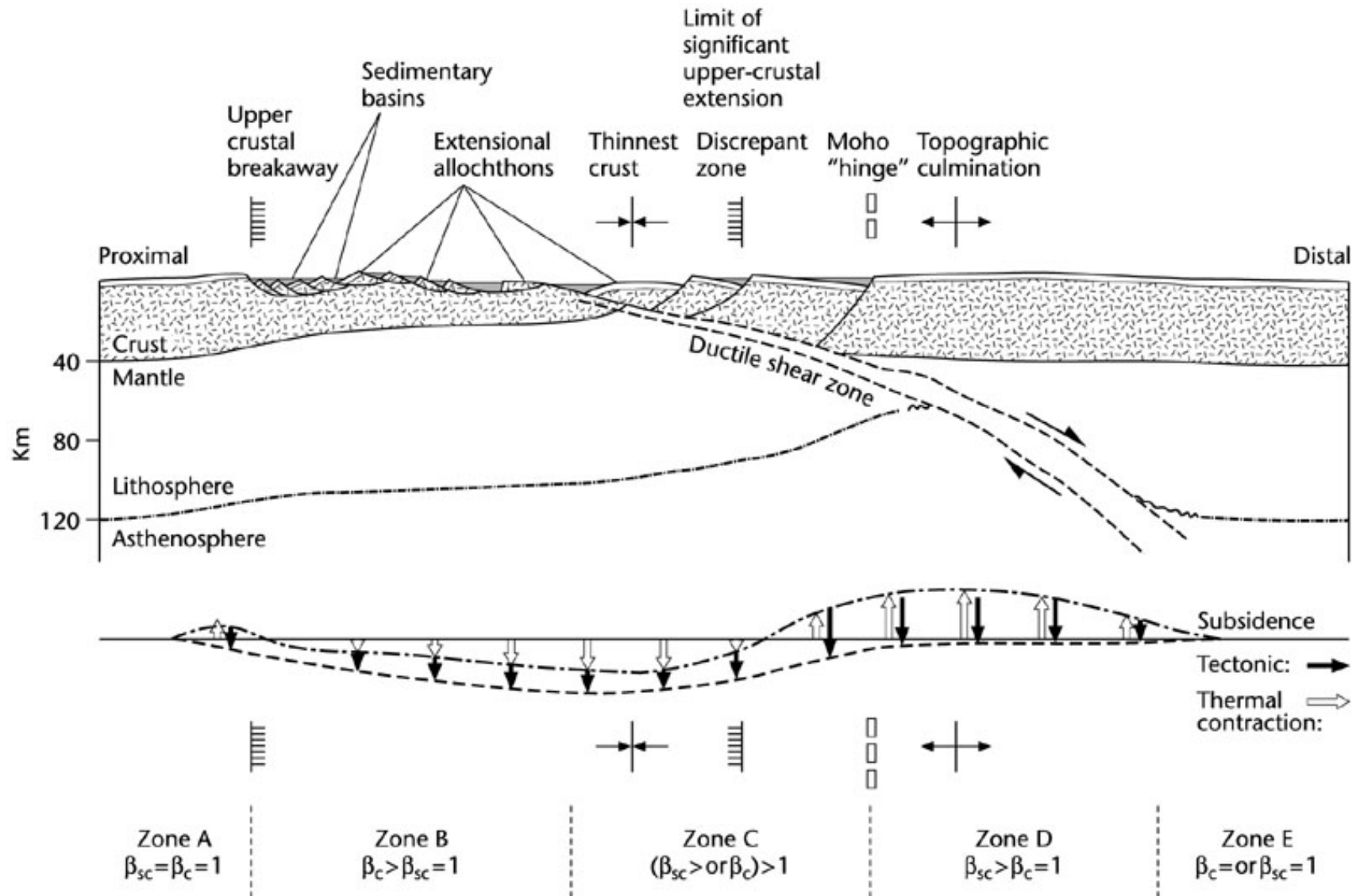
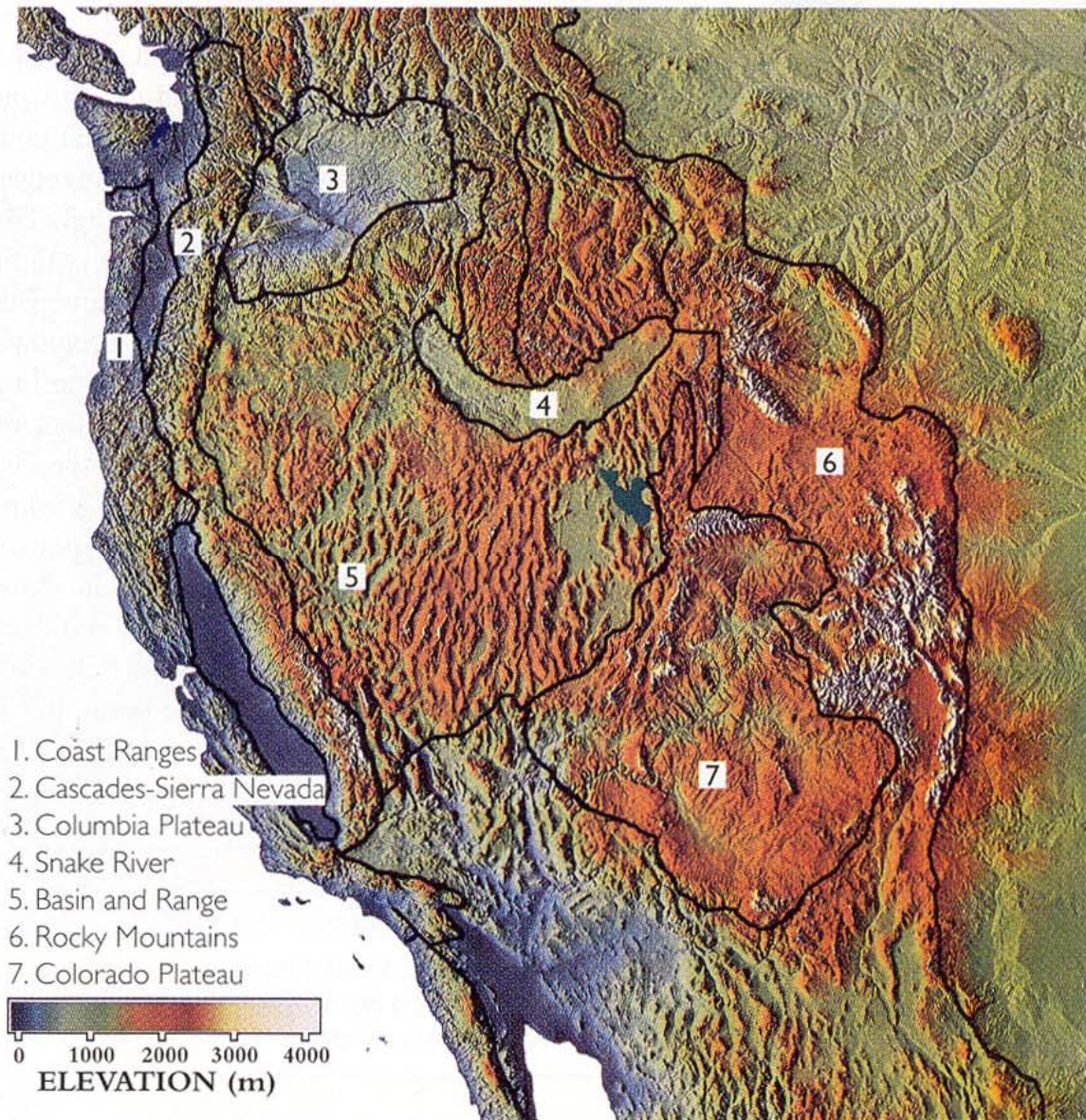


Fig. 3.22 Normal simple shear of the entire lithosphere, developed from the Basin and Range province of SW USA (Wernicke 1985). This geometry takes of the order of 10-15Myr to develop. Midcrustal rocks in the hangingwall may intially pass through greenschist or amphibolite metamorphic conditions in the ductile shear zone, followed by uplift, cooling, and deformation in the brittle field.

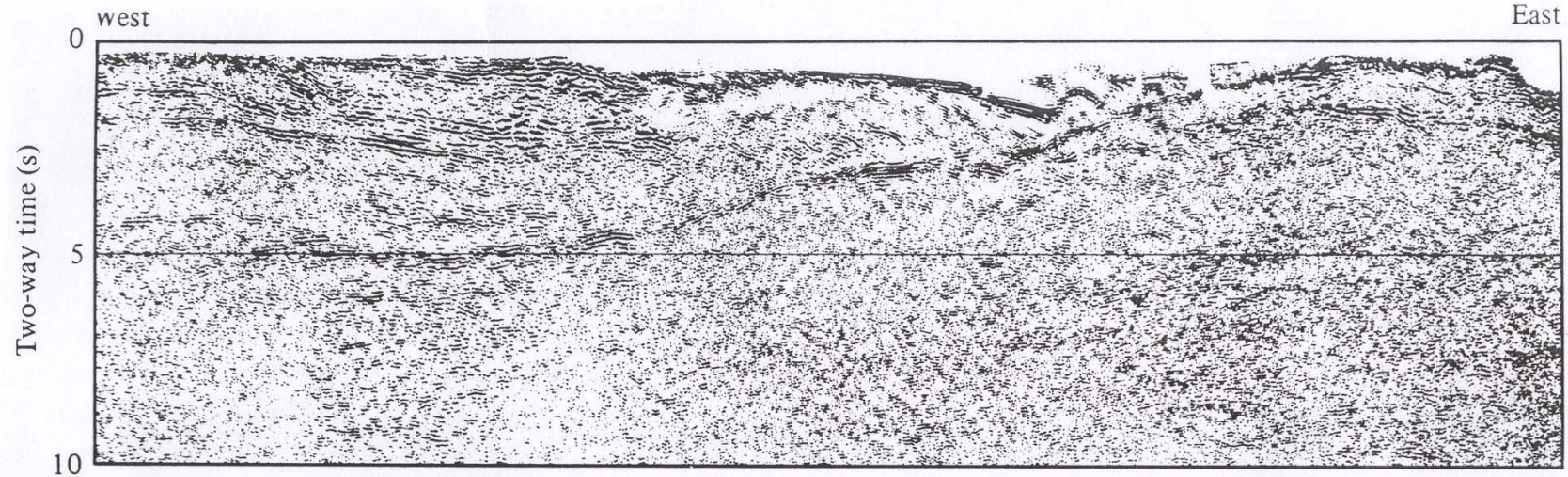
Simple shear (Basin and Range)

Figure 21.8 Color-shaded relief map of the western United States. Computer manipulation of digitized elevation data produced an image in which the major structural provinces and tectonic history of the area are clearly visible, as if illuminated by a light source low in the west. The long, linear ridges of the Basin and Range contrast with the somewhat smoother Colorado Plateau and the rugged and complex relief of the Rocky Mountains and the Cascade and Coast ranges. The low, flat floor of the Snake River is punctuated by individual volcanic cones. The Columbia Plateau stands out as a relatively flat, low-lying basin between the Cascades and the Rocky Mountains. The smooth, sea-level floor of the Great Valley of California is bounded on the east by the Sierra Nevada and on the west by the conspicuous, linear trend of the San Andreas fault system. [Courtesy of David Simpson, IRIS Consortium.]

Press & Siever (2000), p.494



Simple shear (Basin and Range)



Klemperer & Peddy (1992) in *Understanding the Earth: A New Synthesis*.
Brown, Hawkesworth & Wilson (eds), p.264

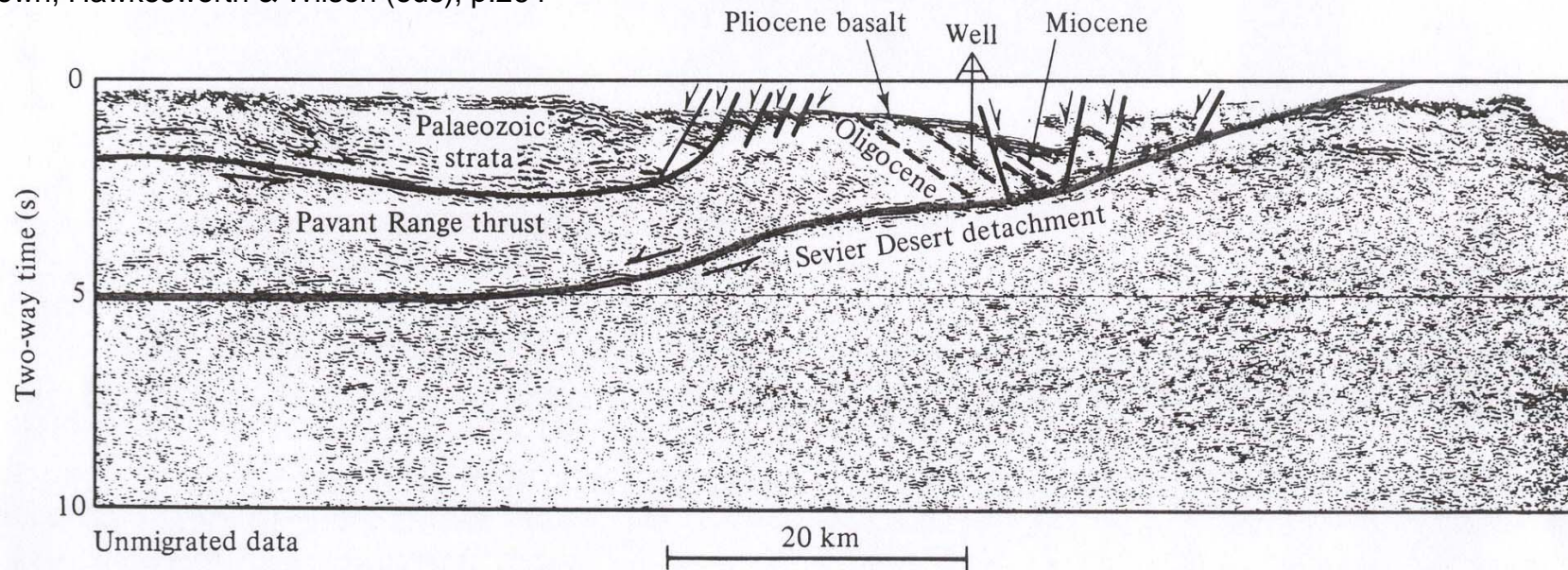
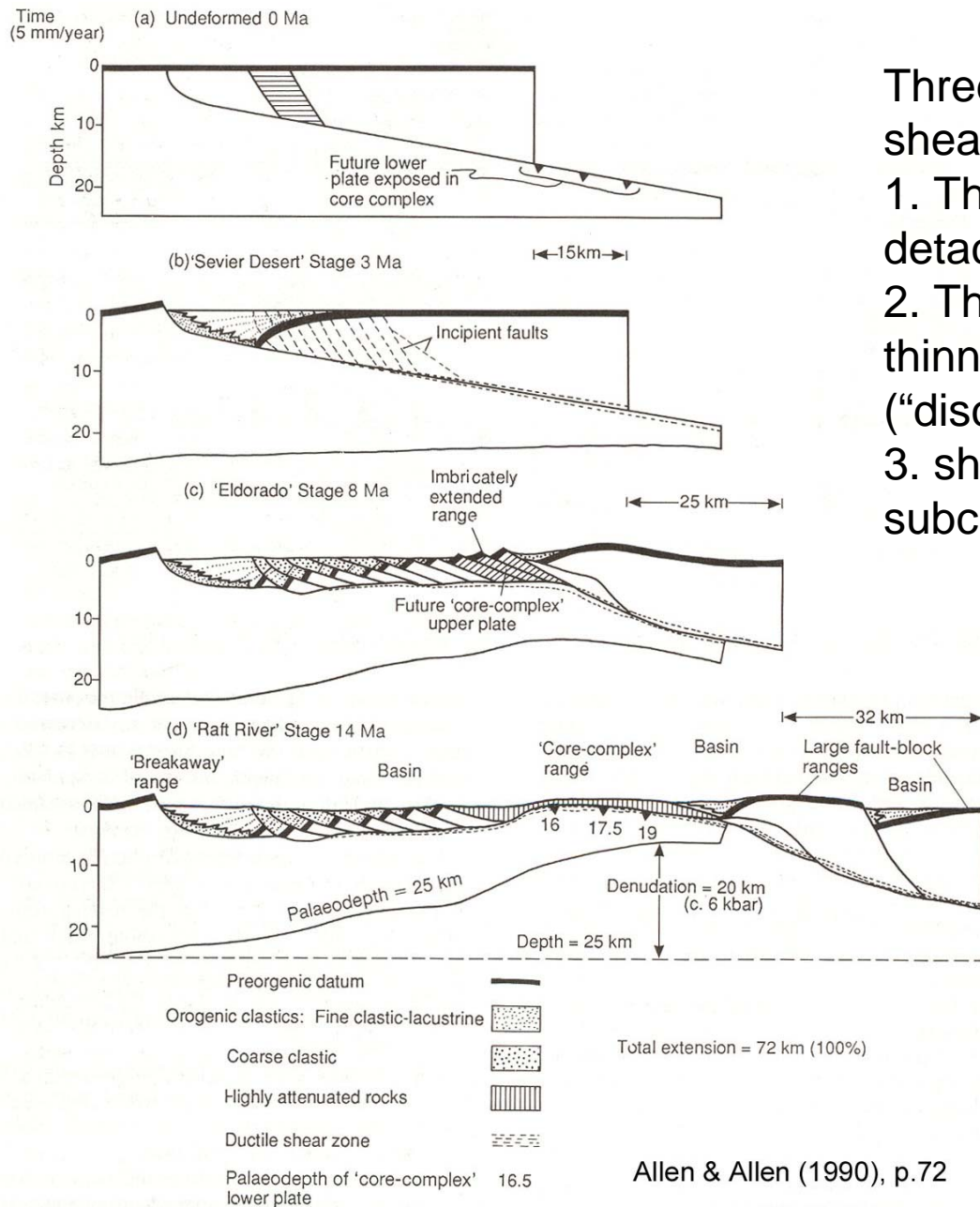


Figure 13.9 COCORP profile across the Sevier Desert detachment, Basin and Range province, uninterpreted and

interpreted data, showing low-angle normal faulting (detachment-style faulting) in the upper crust.



Three zones associated with crustal shear zones:

1. Thinned upper crust above a detachment zone.
2. Thinned lower crust with little thinning in the upper crust ("discrepant" zone).
3. shear zone extends through the subcrustal lithosphere.



Extension Tectonics
in the Basin and Range

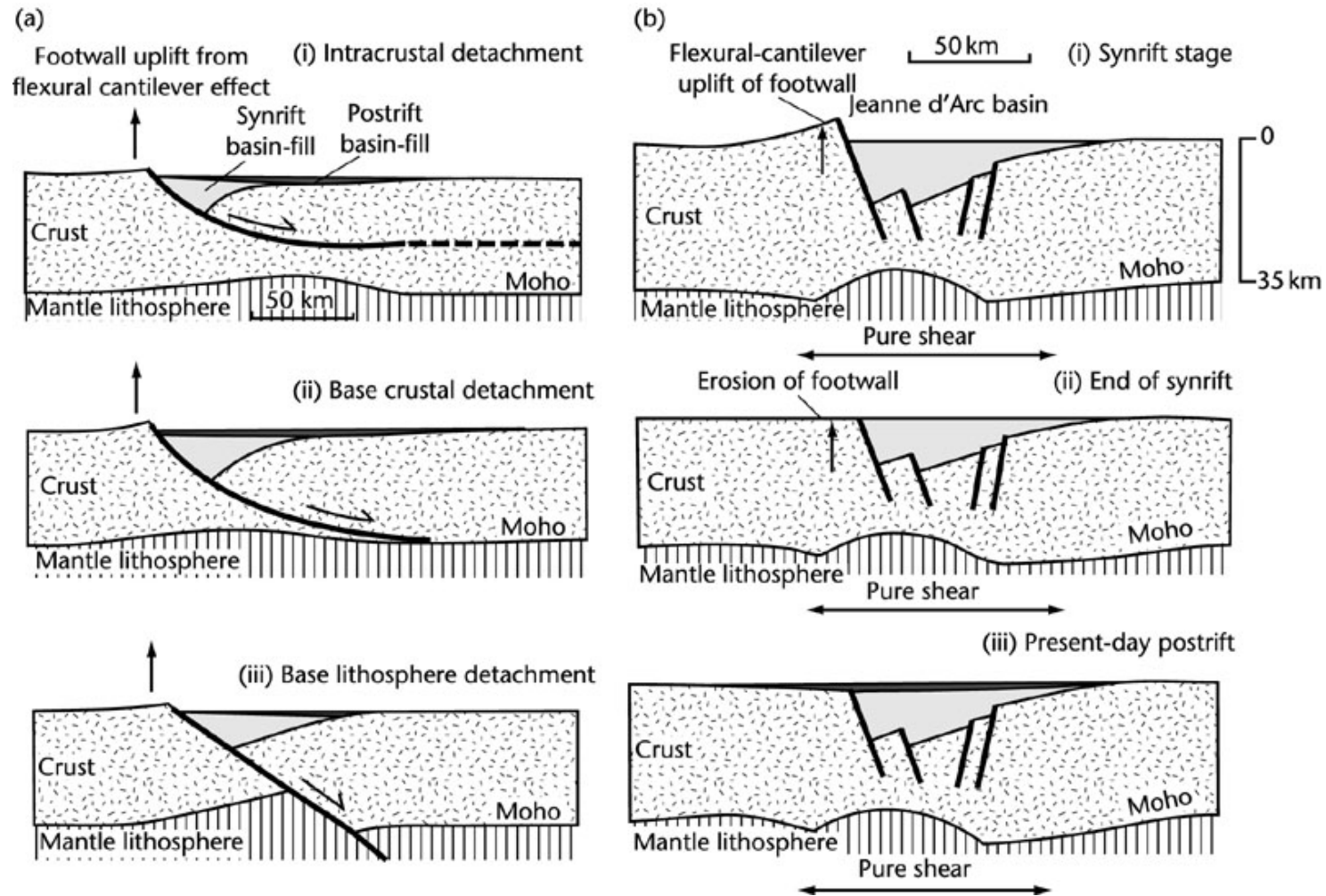


Fig. 3.23 Sedimentary basin geometry and crustal structure predicted by a simple shear-pure shear model including the flexural cantilever effect. (a) Crustal structures after 100 Myr and 30 km extension with an equivalent elastic thickness of 5 km, for an intracrustal detachment (i), a base-crustal detachment (ii), and a base-lithosphere detachment (iii); (b) Sequential development of the Hibernia-Ben Nevis profile of the Jeanne d'Arc basin, showing flexural uplift and erosion of the unloaded footwall of the main detachment fault. The total amount of extension is 18 km, initial fault dip= 60° , initial crustal thickness is 35 km, and $T_e=10$ km.

Tectonic unloading may result in flexural uplift of adjacent footwall areas along major detachment faults – flexural cantilever effect.

3.5.3 Protracted rifting and lateral heat conduction

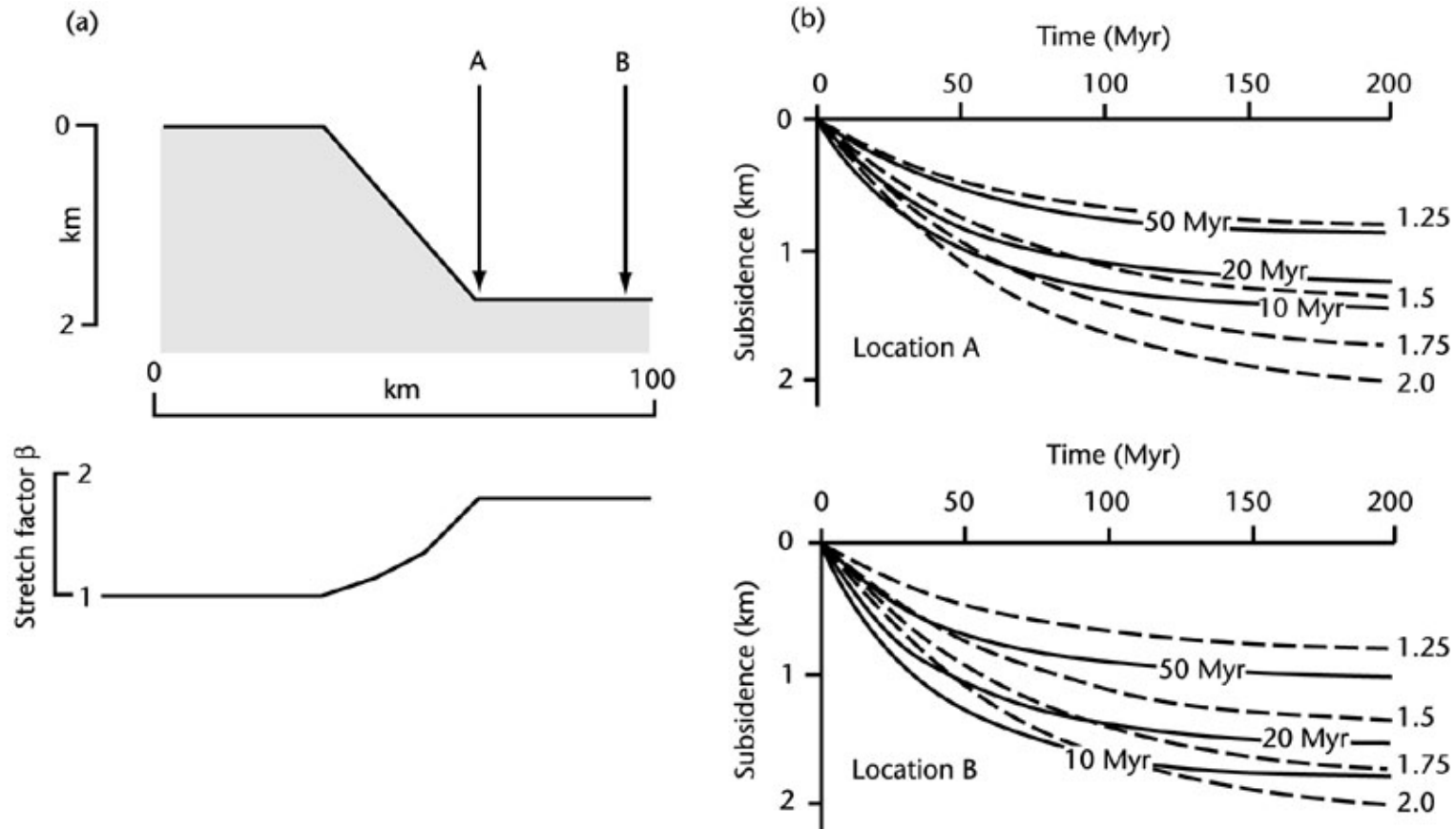


Fig. 3.24 Thermal subsidence for locations A and B in a water-filled basin as a function of time since the end of rifting, for stretch factors of 1.25-2.0, for finite rifting times of 10, 20, and 50 Myr (after Cochran 1983). Dashed lines are subsidence curves for the instantaneous uniform stretching model with $\beta=2$ in the basin centre. Note that the two sets of curves cross-cut, making estimates of the amount of stretching from postrift thermal subsidence problematical unless the duration of stretching is known.